

Privacy-Utility Tradeoffs in Routing Cryptocurrency over Payment Channel Networks

Weizhao Tang
Carnegie Mellon University
wtang2@andrew.cmu.edu

Giulia Fanti
Carnegie Mellon University
gfanti@andrew.cmu.edu

Weina Wang
Carnegie Mellon University
weinaw@cs.cmu.edu

Sewoong Oh
University of Washington
sewoong79@gmail.com

ABSTRACT

Payment channel networks (PCNs) are viewed as one of the most promising scalability solutions for cryptocurrencies today [22]. Roughly, PCNs are networks where each node represents a user and each directed, weighted edge represents funds escrowed on a blockchain; these funds can be transacted only between the endpoints of the edge. Users efficiently transmit funds from node A to B by relaying them over a path connecting A to B, as long as each edge in the path contains enough balance (escrowed funds) to support the transaction. Whenever a transaction succeeds, the edge weights are updated accordingly. However, in deployed PCNs, channel balances (i.e., edge weights) are not revealed to users for privacy reasons; users know only the initial weights at time 0. Hence, when routing transactions, users first guess a path, then check if it supports the transaction. This guess-and-check process dramatically reduces the success rate of transactions. At the other extreme, knowing full channel balances can give substantial improvements in success rate at the expense of privacy. In this work, we study whether a network can reveal *noisy* channel balances to trade off privacy for utility. We show fundamental limits on such a tradeoff, and propose noise mechanisms that achieve the fundamental limit for a general class of graph topologies. Our results suggest that in practice, PCNs should operate either in the low-privacy or low-utility regime; it is not possible to get large gains in utility by giving up a little privacy, or large gains in privacy by sacrificing a little utility.

CCS CONCEPTS

• Security and privacy → Distributed systems security.

KEYWORDS

Blockchain, privacy, p2p network

ACM Reference Format:

Weizhao Tang, Weina Wang, Giulia Fanti, and Sewoong Oh. 2018. Privacy-Utility Tradeoffs in Routing Cryptocurrency over Payment Channel Networks. In *Book Title*. ACM, New York, NY, USA, 18 pages. <https://doi.org/10.1145/1122445.1122456>

1 INTRODUCTION

As the adoption of cryptocurrencies grows to unprecedented levels [4], the scalability limitations of these technologies have become apparent. For example, Bitcoin today can process up to seven transactions per second with a confirmation latency of hours [12, 29]. For comparison, the Visa network can process tens of thousands of transactions per second with a confirmation latency of seconds [26]. This gap raises questions about whether cryptocurrencies are fundamentally able to support as much traffic as traditional, centralized solutions.

In response to these challenges, several cryptocurrencies have turned to a class of scalability solutions called *payment channel networks* (PCNs) [22]. The core idea is that instead of committing every transaction to the blockchain, a separate overlay network (the PCN) is maintained, in which each node represents a user, and each edge represents pre-allocated funds that can be efficiently and quickly transacted between the two endpoints of the edge under a mutual agreement. Critically, those transactions on the PCN are committed to the blockchain only in periodic batches, which reduces the frequency with which users must call the (slow, inefficient) blockchain consensus mechanism. Users can send money to non-adjacent nodes on the PCN by relaying money through intermediate nodes on the graph. PCNs are viewed in the blockchain community as one of the most promising scalability solutions today [13, 25], and several major cryptocurrencies are staking their long-term scaling plans on PCNs. Prominent examples include Bitcoin’s Lightning network [22] and Ethereum’s Raiden network [2].

Despite this excitement, there remain several technical challenges. Principal among them is a privacy-preserving routing problem: each time users wish to route a transaction, they must find a path through the PCN with enough pre-allocated funds to route the transaction. However, in today’s PCNs, edge balances are not publicly revealed for privacy reasons, making it difficult to find such a route reliably. The goal of this paper is to study privacy-utility tradeoffs that arise in such a PCN transaction routing. Before defining the problem more precisely, we begin with a brief primer.

Permission to make digital or hard copies of all or part of this work for personal or classroom use is granted without fee provided that copies are not made or distributed for profit or commercial advantage and that copies bear this notice and the full citation on the first page. Copyrights for components of this work owned by others than ACM must be honored. Abstracting with credit is permitted. To copy otherwise, or republish, to post on servers or to redistribute to lists, requires prior specific permission and/or a fee. Request permissions from permissions@acm.org.

Woodstock '18, June 03–05, 2018, Woodstock, NY

© 2018 Association for Computing Machinery.

ACM ISBN 978-1-4503-9999-9/18/06...\$15.00

<https://doi.org/10.1145/1122445.1122456>

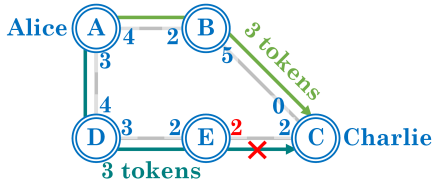


Figure 1: Payment channel network. Alice wants to send 3 tokens to Charlie. Transaction fees are omitted for simplicity.

1.1 Payment Channel Networks (PCNs)

A *payment channel* is a transaction between two parties that escrows currency for use only between those two parties for some amount of time. For example, Alice and Bob could escrow 4 and 2 tokens, respectively, for the next week. The escrow transaction is committed to the blockchain to finalize it. Once the channel is finalized, Alice and Bob can send escrowed funds back and forth by digitally signing the previous state of the channel and the new updated transaction. For example, Alice can send 3 of her 4 tokens to Bob, so that the new channel state is (Alice=1, Bob=5). Once the parties decide to close the channel, they can commit its final state through another blockchain transaction. Cryptographic and incentive-based protections prevent users from stealing funds in a channel, e.g., by committing an outdated state. Maintaining a payment channel has an opportunity cost because users must lock up their funds while the channel is active, and they are not actually paid until the channel is closed. Hence, it is not practical to expect users to maintain a channel with every individual with whom they may ever need to transact.

A *payment channel network* (PCN) gets around this problem by setting up a graph of bidirectional payment channels. The key idea is that if Alice wants to transact with Charlie, but is only connected to him via Bob, then Bob can act as a relay for Alice’s money, passing it along to Charlie. Again, cryptographic protections are used to ensure that Bob does not steal Alice’s relayed money, but he does receive a small fee as payment for his cooperation. Notice that if Alice wants to send r tokens to any node in the network, she must first find a directed path to that node with at least r tokens on every (directed) edge. For example, in Figure 1, suppose Alice wants to send $r = 3$ tokens to Charlie. She has two paths available: $A \rightarrow B \rightarrow C$ and $A \rightarrow D \rightarrow E \rightarrow C$. However, the edge $E \rightarrow C$ has only 2 tokens to send in that direction, so it cannot support Alice’s transaction. Hence, this transaction fails. Suppose Alice instead sends her transaction over the first path, $A \rightarrow B \rightarrow C$. After her transaction is processed, each of the channels moves $r = 3$ tokens (plus a small processing fee) from one side of the channel to the other. Note that one could also packet-switch transactions, so Alice sends part of her transaction over multiple paths. In today’s PCNs, this functionality is not yet implemented [1]; however, such routing schemes can give significant performance enhancements [10, 15, 21, 24]. Packet-switched routing is beyond our scope.

Our work studies the act of finding a path from source to destination with sufficient balance to support a transaction. If the full graph and edge weights were known, finding such a path would

be straightforward (albeit computationally-intensive). However, if users were given access to instantaneous channel balances of the whole network, any passive observer could trivially see that, for instance, r tokens flowed along a path from Alice to Charlie. This is a serious breach of privacy.

Today’s PCNs do not reveal instantaneous balance information in an attempt to prevent observers from inferring other users’ transaction patterns. Instead, users are given access only to the graph topology, and the *sum* of balances in either direction on each channel, which remains constant for the duration of the channel. Because of this design decision, PCN users are forced to guess if a given path has enough balance to support a particular transaction by attempting to send their transaction over that path. If it fails, the user tries another path until the transaction either completes or times out; upon a timeout, the user can instead process her transaction on the blockchain, which is comparatively slow and expensive. This guess-and-check routing approach uses unnecessary resources and severely limits the success rates of today’s PCNs [27]. Every time a user tries to route over a path that will ultimately fail, it temporarily ties up funds along that path, which cannot be used by other transactions. Moreover, since users are forced to guess channel balances, they are more likely to not find any valid path prior to transaction timeout. Our goal in this work is to understand whether privacy must always come at such a high cost. In particular, we consider whether a system could reveal *noisy* channel balances in an effort to gracefully trade off privacy for utility.

1.2 Contributions

Our contributions are threefold:

- We theoretically model the routing problem in PCNs and define distribution-free metrics for privacy and utility. We show a so-called *diagonal* upper bound on the privacy-utility tradeoff for these metrics over general graphs and a significant class of shortest-path transaction routing strategies. We show that the diagonal bound is tight by designing noise mechanisms that achieve it.
- The diagonal bound is a somewhat negative result, suggesting that a good tradeoff is not possible. However, we show that by relaxing certain assumptions (e.g., the shortest-path routing assumption), we can break the diagonal barrier. Indeed, one can design noise mechanisms that asymptotically achieve a perfect privacy-utility tradeoff. However, this comes at the cost of increasingly long paths, i.e., increasingly expensive routing fees.
- We demonstrate through simulation that even if one were to consider an average-case utility metric (fraction of successful transactions, or success rate) rather than a worst-case one, the privacy-success rate tradeoff is still not favorable for shortest-path routing. We use simulation to uncover real-world effects like deadlocks, which can occur because of noisy balance information. Overall, our simulations suggest that trading off privacy for utility does not give significant gains unless the system operates either in a low-privacy regime or low-utility regime; today’s PCNs operate in the low-utility regime.

In sum, our results suggest that PCNs may not be able to provide utility and privacy simultaneously. Moreover, our theoretical analysis is conducted under an adversarial model that (a) is passive,

and (b) does not exploit temporal correlations in transaction patterns. Hence, actual privacy threats are likely even more dire than our results indicate. PCN system designers may therefore need to make an explicit choice regarding whether the value of PCNs comes mainly from their potential for improving performance or privacy, and choose an operating point accordingly.

2 MODEL

We model the PCN as a graph $\mathcal{G}(\mathcal{V}, \mathcal{E})$, where \mathcal{V} denotes the participating nodes with $n = |\mathcal{V}|$, and \mathcal{E} the set of edges, or payment channels, in the PCN. Each edge $(u, v) \in \mathcal{E}$ is associated with two weights, b_{uv} and b_{vu} , which denote the balances from u to v and from v to u , respectively. The *capacity* of the channel, denoted as $C_{uv} = b_{uv} + b_{vu}$, is assumed to be a constant; this models a setting where the channel remains open for the entire duration of the experiment. Recall that our goal is to release noisy channel balances, so the true balances may not be equal to the publicly-released channel balances, which we denote by \tilde{b}_{uv} and \tilde{b}_{vu} , respectively.

We assume an arbitrary sequence of transactions x_1, x_2, \dots enters the system sequentially. Each transaction x_i has an associated source $s(x_i)$, destination $d(x_i)$, amount $r(x_i)$, and timestamp $t(x_i)$, where $t(x_i) < t(x_{i+1})$ for all i . Each transaction is processed instantaneously at its time-of-arrival timestamp. That is, we do not account for concurrent transactions. For a path P on the graph, we use $s(P)$ and $d(P)$ to denote its source and destination, respectively. At transaction x 's time of arrival, $t(x)$, the source $s(x)$ chooses a path P from the network with source $s(P) = s(x)$ and destination $d(P) = d(x)$, such that P appears to have enough balance according to the publicly visible balances. That is, $\forall (u, v) \in P, \tilde{b}_{uv} \geq r(x)$. Recall that channel balances are noisy, so a path that appears to have enough balance may not in reality.

If the path chosen for transaction x does not have enough balance (i.e., $\exists (u, v) \in P : \tilde{b}_{uv} < r(x)$), the transaction fails. In this case, both the visible channel balances \tilde{b}_{uv} and the true channel balances b_{uv} remain unchanged. If the path chosen for transaction x has enough balance (i.e., $\forall (u, v) \in P, \tilde{b}_{uv} \geq r(x)$), the transaction succeeds, and $\forall (u, v) \in P$, the true channel balance is updated as $b_{uv} = \tilde{b}_{uv} - r(x)$ and $b_{vu} = \tilde{b}_{vu} + r(x)$. The visible channel balances, on the other hand, are updated according to a *noise mechanism* (or *mechanism*). The noise mechanism is probabilistic and chosen by the system designer; given an input path P , it outputs a random set of edges $Q \subseteq P$ such that $\forall (u, v) \in Q$, the public balance \tilde{b}_{uv} is updated to the true new balance, b_{uv} . We denote this conditional probability distribution by $\mathbb{D}[Q|P]$.

Notice two things about this model: first, we never update public balances on edges that were not involved in a transaction, i.e., edges that are not elements of path P . This modeling choice was made in part for analytical tractability and in part for practicality; since nodes anyway must communicate with all relays in P , it is easy to include an instruction for the noisy balance update. Reaching other nodes would require additional communication that may not be practical. Second, note that if an edge is updated, it is only updated to its true balance—never a noisy version of its balance. One could additionally impose the condition that after choosing a subset Q , the noise mechanism updates the balances in Q by different amounts (not necessarily equal to $r(x)$); however, as we will discuss

in Section 2.1, our privacy metric only considers adversaries who aim to identify the source or destination of a transaction—not the amount. Hence, if an adversary observes *any* update on an edge, it knows that edge was involved in the transaction; knowing the exact amount does not give any more information about the source or destination. Hence, to maximize utility, we might as well reveal the full balance update.

2.1 Privacy Metric

Our adversary is an honest-but-curious user that passively observes the network and tries to infer the source and destination of the first transaction x to pass through the system; the adversary does *not* try to guess the transaction amount $r(x)$. We assume that the initial public balances are all identical to the real balances, i.e., $\forall (u, v) \in \mathcal{E}, b_{uv} = \tilde{b}_{uv}$ at time 0, and all the balances in the PCN are sufficient to support x ; hence, this metric is equivalent to considering an arbitrary transaction x but giving the adversary knowledge of the true balances shortly before $t(x)$. More precisely, once x has been processed, the adversary guesses one node $v \in \mathcal{V}$ with probability $\mathbb{A}[v|Q]$, where \mathbb{A} is a randomized adversarial strategy. If $v \in \partial P$, where $\partial P \triangleq \{s(P), d(P)\}$, i.e., if the adversary guesses the source or destination correctly, it wins. To avoid making assumptions about the transaction or PCN distribution, we consider a worst-case metric over both. As shown in (2.1), privacy is defined as the minimax probability that the adversary makes a wrong estimate:

$$\begin{aligned} \Pi(\mathbb{D}) &= 1 - \sup_{\mathbb{A}} \min_{P \in \mathcal{P}} \sum_{v \in \partial P, Q \subseteq P} \mathbb{D}[Q|P] \mathbb{A}[v|Q] \\ &= 1 - \sup_{\mathbb{A}} \min_{P \in \mathcal{P}} \sum_{Q \subseteq P} \mathbb{D}[Q|P] \mathbb{A}[\partial P|Q], \end{aligned} \quad (2.1)$$

where \mathcal{P} denotes the set of paths in \mathcal{G} . For convenience, we let $\mathbb{A}[\partial P|Q]$ denote $\sum_{v \in \partial P} \mathbb{A}[v|Q]$.

Notice that $\mathbb{A}[\cdot|Q]$ is a probability distribution with event space \mathcal{V} , i.e. the supremum over \mathbb{A} is taken in the space

$$\mathcal{A} = \left\{ \mathbb{A} \mid \forall u \in \mathcal{V}, P \in \mathcal{P}, Q \subseteq P : \mathbb{A}[u|Q] \geq 0, \sum_{v \in \mathcal{V}} \mathbb{A}[v|Q] = 1 \right\}.$$

So constraint $\mathbb{A} \in \mathcal{A}$ is an intersection of linear constraints. In addition, the objective of (2.1) is the minimum of finite number of affine functions of \mathbb{A} . Hence, the optimization problem in (2.1) is equivalent to an LP. Because \mathcal{A} is compact, the supremum of the optimization problem is attained. However, solving this optimization is intractable in general, due to the optimization over all the paths in the PCN. We will show that under certain restrictions, a solution can be computed efficiently.

2.2 Utility Metric

The performance of a PCN is commonly measured by its *success rate*, or the fraction of transactions it successfully processes [18, 23, 24]. However, expected success rate is a complicated function that depends on transaction workloads, graph topology, and initial balances. Since we wish to avoid making assumptions on these characteristics, we instead consider a simpler notion of utility: how representative are the observed balances of the true underlying balances? Specifically, given the true balance of a link, we consider

the probability that the observed balance is equal to the true balance, which we will refer to as the *truthful probability*. In general, this probability for a given PCN still depends on the transaction workload, as well as parameters like the path length. Hence, we consider a *worst-case* transaction workload that minimizes the truthful probability.

To this end, we define the quantity in (2.2) below as the utility of mechanism \mathbb{D} . It equals the minimum probability, over all paths and edges in paths, of a public edge balance equaling the true edge balance after a transaction passes through it:

$$U(\mathbb{D}) = \min_{P \in \mathcal{P}} \min_{\epsilon \in P} \sum_{Q: Q \ni \epsilon, Q \subseteq P} \mathbb{D}[Q|P] \quad (2.2)$$

In the proposition below, we show how this notion of utility is related to the truthful probability.

PROPOSITION 2.1. *The truthful probability of any edge given any value of the true balance is lower bounded by the utility $U(\mathbb{D})$.*

Proof. We focus on a particular edge $\epsilon \in \mathcal{E}$. Assume at the current state, the true and public balances of ϵ are B_ϵ , \tilde{B}_ϵ , respectively. Define event

$E_\epsilon \triangleq$ there exists a previous transaction going through ϵ .

If $\neg E_\epsilon$ happens, then $\mathbb{P}[B_\epsilon = \tilde{B}_\epsilon | \neg E_\epsilon] = 1$, since both balances are identical to their initial states, at which time all public balances are truthful.

If E_ϵ happens, we focus on the state when the last transaction T_{-1} on path P' involving ϵ was about to be launched. At this state, we assume the true and public balances of ϵ are b_ϵ and \tilde{b}_ϵ , while they have been B_ϵ and \tilde{B}_ϵ since T_{-1} was launched, respectively. By definition of utility,

$$U(\mathbb{D}) \leq \sum_{Q: Q \ni \epsilon, Q \subseteq P'} \mathbb{D}[Q|P'] = \mathbb{P}[\tilde{B}_\epsilon = B_\epsilon | E_\epsilon, T_{-1}].$$

Since T_{-1} could be arbitrary, $\mathbb{P}[\tilde{B}_\epsilon = B_\epsilon | E_\epsilon] \geq U(\mathbb{D})$.

To summarize, $\mathbb{P}[B_\epsilon = \tilde{B}_\epsilon] \geq U(\mathbb{D})$ holds for all $\epsilon \in \mathcal{E}$ regardless of previous workload on the network. \square

From the proof of Proposition 2.1, we can also see that $U(\mathbb{D})$ is *equal* to the truthful probability of an edge ϵ in the following scenario: a transaction happens along a path P' that contains ϵ , and ϵ and P' are the minimizers in the definition of $U(\mathbb{D})$. Therefore, $U(\mathbb{D})$ fully characterizes the truthful probability in a worst-case sense. For this reason, we will focus on $U(\mathbb{D})$ as our utility metric.

3 FUNDAMENTAL LIMITS

As system designers, we want the the privacy and utility metrics defined in (2.1) and (2.2) to be high, i.e., close to 1. In this section, we show that for an important class of routing algorithms, this is not possible; additionally, we provide a tight upper bound on the tradeoff between these quantities.

Let us begin by considering two extreme points. First, consider a setting with perfect utility, $U(\mathbb{D}) = 1$. To achieve perfect utility, on every path, the balance of every edge must be truthfully updated. Hence, if the adversary simply guesses the source of of the observed updated path, it always wins, so we have no privacy: $\Pi(\mathbb{D}) = 0$.

Next, consider a case with no utility, $U(\mathbb{D}) = 0$. This implies that for every path, noise mechanism \mathbb{D} always hides the balance update

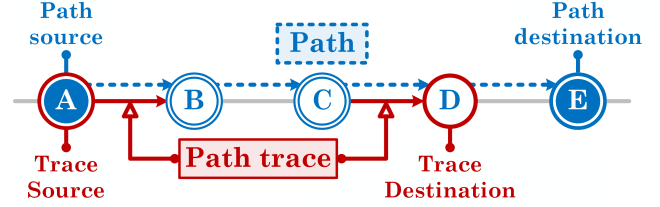


Figure 2: Example of a path from A to E and a corresponding path trace, the set of edges $A \rightarrow B$ and $C \rightarrow D$.

on at least one edge from the true path. Regardless of the noise mechanism, the adversary can always pick a node uniformly at random. Since there are n nodes, it guesses the source or destination with probability $2/n$, so $\Pi(\mathbb{D}) \leq 1 - \frac{2}{n}$, $\forall \mathbb{D}$. Hence, we have an upper bound on the privacy metric at the two extremes of the utility spectrum.

The more challenging and interesting case arises when $0 \leq U(\mathbb{D}) \leq 1$. We first define a *path trace*, which intuitively describes a (possibly disjoint) set of edges that are elements of a path between two endpoints. This set of edges must include the first and last hop of the path, adjacent to the two endpoints (Figure 2).

Definition 3.1. Given two nodes x and y on an arbitrary undirected graph $(\mathcal{V}, \mathcal{E})$ with set of available paths \mathcal{P} , a set of oriented edges Q is a **path trace** from x to y , if and only if

- (1) x has an incident edge in Q with x being the source;
- (2) y has an incident edge in Q with y being the destination;
- (3) there exists a path $P \in \mathcal{P}$, $P \supseteq Q$ from x to y .

We say x is a **source** of Q , and y is a **destination** of Q .

In other words, a path trace is what the adversary sees after the noise mechanism updates a subset of edges in a given path. A path trace is always a subset of an available path in \mathcal{P} . Our first main result, Theorem 3.2, states that if \mathcal{P} includes only shortest paths between nodes, then the privacy metric is upper bounded by a linear relation that we call the *diagonal bound*. Notice that shortest-path routing is extremely common. First, today's PCNs like the Lightning network implement shortest-path routing by default [1]. Second, since intermediate relays in PCNs extract transaction fees, shortest-path routing can be thought of as a proxy for cheapest routing, which users are incentivized to use. Hence this result applies to the vast majority of routes used in practice.

THEOREM 3.2 (THE DIAGONAL BOUND). *On a network $(\mathcal{V}, \mathcal{E}, \mathcal{P})$ with $n = |\mathcal{V}| \geq 2$, if \mathcal{P} includes only shortest paths, then for any noise mechanism \mathbb{D} , its privacy $\Pi(\mathbb{D})$ and utility $U(\mathbb{D})$ satisfy*

$$\Pi(\mathbb{D}) \leq \left(1 - \frac{2}{n}\right) [1 - U(\mathbb{D})]. \quad (3.1)$$

Notice that this bound, plotted in Figure 3, does not make assumptions about the structure of the underlying graph. Intuitively, the result holds because for any observed path trace taken from a shortest path between two nodes on an arbitrary graph, the adversary can uniquely identify its source and destination. For example, consider Figure 4 (left). On a tree, even if the noise mechanism reveals only a subset of edges in a path, the adversary can trivially

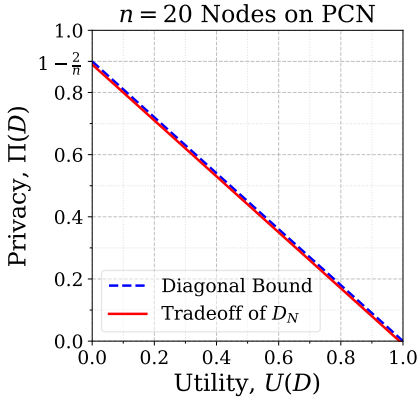


Figure 3: The diagonal upper bound of Theorem 3.2, and the achievable tradeoff for the all-or-nothing scheme. The all-or-nothing curve is slightly displaced from the upper bound for greater visibility.

reconstruct the interior path exactly. From this reconstruction, the endpoints are clear. Notice that in a path trace, we know the orientation of each edge because a truthfully-updated channel will always reveal the direction of money flow. In Figure 4 (right), we see that on a grid graph, the adversary cannot always reconstruct the exact path, as there may be multiple shortest paths consistent with the path trace. For instance, the adversary cannot tell if $B \rightarrow C \rightarrow E$ or $B \rightarrow D \rightarrow E$ was the true path. However, the adversary *can* uniquely determine the set of endpoints of the trace: A and E . Any other choice (e.g. A and D) that passes through the full set of path trace edges has a strictly longer path length. This observation is true for general graphs, allowing the adversary to use the source or destination of the path trace as its estimate of the source or destination of the original path. This in turn causes the privacy metric for a noise mechanism to be governed primarily by its behavior near the source and destination, giving rise to the diagonal bound.

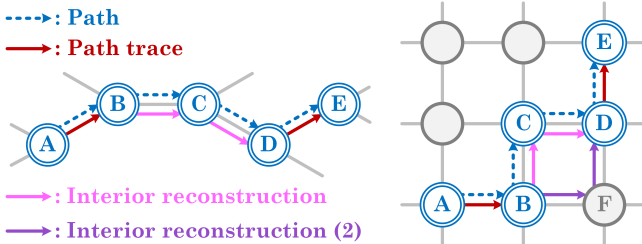


Figure 4: Examples of a path and a path trace on a 3-regular tree (left) and a grid graph (right), assuming shortest-path routing. For a tree, given any path trace, we can always uniquely determine the path that generated the path trace (up to the endpoints of the path trace). On a grid graph (indeed, on general graphs), we can uniquely determine the endpoints of the path trace, but not necessarily the full path.

Proof. First, given that all routes are shortest paths, we prove the claim that there exists a unique pair of source and destination nodes of any path trace $Q \subseteq \mathcal{E}$. Let $\delta(u, v)$ denote the distance between any pair of nodes u, v on the graph. Assume by contradiction that Q is a path trace from x to y , and from z to w , where $\{x, y\} \neq \{z, w\}$. By definition, there exist paths P_{zw} and P_{xy} , where

- (1) The endpoints of P_{zw} are z and w ;
- (2) The endpoints of P_{xy} are x and y ;
- (3) Q is a subset of both P_{zw} and P_{xy} .

As a result, both x and y are on path P_{zw} . Because P_{zw} is the shortest path connecting z and w , its segment connecting x and y is also the shortest path connecting x and y . Since $\{x, y\}$ is different from $\{z, w\}$, we have $\delta(x, y) < \delta(z, w)$. By the same reasoning, we get $\delta(z, w) < \delta(x, y)$ from z, w belonging to path P_{xy} , which is a contradiction. Therefore, any path trace $Q \subseteq \mathcal{E}$ with a source has a unique source. So there exists a function $s : 2^{\mathcal{E}} - \{\emptyset\} \rightarrow \mathcal{V}$, mapping each path trace to its source. Define $s(\emptyset) \notin \mathcal{V}$.

To upper bound our privacy metric, we will analyze the privacy achievable by an adversary with strategy \mathbb{A}_N , where

- (1) If no edge is updated by the noise mechanism, the adversary guesses randomly, i.e. $\mathbb{A}_N[v|\emptyset] = \frac{1}{n}$ for all $v \in \mathcal{V}$;
- (2) If a set of edges $Q \neq \emptyset$ is updated, the adversary estimates its source, i.e. $\mathbb{A}_N[s(Q)|Q] = 1$.

Let $\varepsilon_s(P)$ denote the first edge of path P . By our privacy definition,

$$\begin{aligned} \Pi(\mathbb{D}) &= 1 - \sup_{\mathbb{A}} \min_{P \in \mathcal{P}} \sum_{Q \subseteq P} \mathbb{D}[Q|P] \mathbb{A}[\partial P|Q] \\ &\leq 1 - \min_{P \in \mathcal{P}} \sum_{Q \subseteq P} \mathbb{D}[Q|P] \mathbb{A}_N[\partial P|Q] \\ &= 1 - \min_{P \in \mathcal{P}} \left[\frac{2\mathbb{D}[\emptyset|P]}{n} + \sum_{Q:s(Q)=s(P), Q \subseteq P} \mathbb{D}[Q|P] \right], \end{aligned} \quad (3.2)$$

where the last equality comes from splitting the adversary's probability of success into random guessing if no edges are updated, plus the probability of the noise mechanism revealing a path trace that truthfully reveals the true source edge. Recall that $\mathbb{A}[\partial P|Q]$ denotes the adversary's probability of guessing one of the endpoints of P upon observing path trace Q .

Because $\mathbb{D}[\cdot|P]$ is a probability distribution, the following constraints hold.

$$\begin{aligned} \mathbb{D}[\emptyset|P] + \sum_{Q:s(Q)=s(P), Q \subseteq P} \mathbb{D}[Q|P] &\leq 1; \\ \sum_{Q:s(Q)=s(P), Q \subseteq P} \mathbb{D}[Q|P] &= \sum_{Q:Q \ni \varepsilon_s(P), Q \subseteq P} \mathbb{D}[Q|P] \geq U(\mathbb{D}), \end{aligned}$$

where the latter condition follows from the definition of utility. If we assume $n \geq 2$, it follows that for any P ,

$$\frac{2\mathbb{D}[\emptyset|P]}{n} + \sum_{Q:s(Q)=s(P), Q \subseteq P} \mathbb{D}[Q|P] \geq \frac{2}{n}[1 - U(\mathbb{D})] + U(\mathbb{D}).$$

By substituting it back to (3.2), we obtain

$$\Pi(\mathbb{D}) \leq 1 - U(\mathbb{D}) - \frac{2}{n}[1 - U(\mathbb{D})],$$

which is equivalent to (3.1). \square

We next prove that the bound in Theorem 3.2 is tight. The proof of the upper bound implies that hiding edges in the interior of a path does not improve privacy if one or both of the endpoints of the path are revealed. In other words, an adversary cannot always determine the sequence of edges between the endpoints of a path trace, but it can identify the *endpoints* of the trace. Because there is no privacy benefit to hiding interior edges of a path, we should maximize utility (for a given privacy level) by revealing all interior edges. This motivates the so-called *all-or-nothing* noise mechanism.

Definition 3.3. For a transaction routed over path P , the **all-or-nothing noise mechanism** \mathbb{D}_N either truthfully updates balance on every edge of P with probability $U(\mathbb{D}_N)$, or updates nothing with probability $1 - U(\mathbb{D}_N)$.

We define a *reachable* network as follows:

Definition 3.4. A network $(\mathcal{V}, \mathcal{E}, \mathcal{P})$ is **reachable**, if for any pair of nodes $(u, v) \in \mathcal{V}^2$ with $u \neq v$, there exists a path $P \in \mathcal{P}$ that goes from u to v , or from v to u .

LEMMA 3.5. *On a reachable network,*

$$\sup_{\mathbb{A}[\cdot|\varnothing]} \min_{P \in \mathcal{P}} \mathbb{A}[\partial P|\varnothing] = \frac{2}{n}. \quad (3.3)$$

Proof. Because $\mathbb{A}[\cdot|\varnothing]$ is a probability distribution, for any strategy \mathbb{A} , there exists 2 nodes u_1, u_2 such that

$$\mathbb{A}[u_1|\varnothing] + \mathbb{A}[u_2|\varnothing] \leq \frac{2}{n}.$$

By assumption that the network is reachable, there exists a path P_u connecting u_1, u_2 . Hence,

$$\min_{P \in \mathcal{P}} \mathbb{A}[\partial P|\varnothing] \leq \mathbb{A}[\partial P_u|\varnothing] \leq \frac{2}{n}, \quad \forall \mathbb{A}.$$

In the meantime, the adversary who guesses each node uniformly could make the inequality above tight, which proves (3.3). \square

On a reachable network, the below theorem characterizes the privacy-utility tradeoff for the all-or-nothing noise mechanism.

THEOREM 3.6. *On a reachable network, the privacy-utility tradeoff of the all-or-nothing noise mechanism is characterized by*

$$\Pi(\mathbb{D}_N) = \left(1 - \frac{2}{n}\right) [1 - U(\mathbb{D}_N)]. \quad (3.4)$$

Although this result holds for all reachable networks, regardless of routing policy, it also implies that the upper bound in Theorem 3.2 is tight for shortest-path routing over reachable networks.

Proof. When the entire path is updated, the adversary \mathbb{A}_0 may directly pick an endpoint of the observed path as its estimate. Hence,

$$\sup_{\mathbb{A}} \min_{P' \in \mathcal{P}} \mathbb{A}[\partial P'|P'] = \mathbb{A}_0[\partial P|P] = 1, \quad \forall P \in \mathcal{P}.$$

By our privacy definition,

$$\begin{aligned} \Pi(\mathbb{D}_N) &= 1 - \sup_{\mathbb{A}} \min_{P \in \mathcal{P}} \sum_{Q \subseteq P} \mathbb{D}_N[Q|P] \mathbb{A}[\partial P|Q] \\ &= 1 - \sup_{\mathbb{A}} \min_{P \in \mathcal{P}} \{[1 - U(\mathbb{D})] \mathbb{A}[\partial P|\varnothing] + U(\mathbb{D}) \mathbb{A}[\partial P|P]\} \\ &= [1 - U(\mathbb{D})] \left(1 - \sup_{\mathbb{A}} \min_{P \in \mathcal{P}} \mathbb{A}[\partial P|\varnothing]\right) \end{aligned}$$

$$= [1 - U(\mathbb{D})] \left(1 - \frac{2}{n}\right). \quad (*)$$

Obtained by Lemma 3.5, (*) justifies the original claim. \square

The results of this section are not encouraging; they imply that a perfect privacy-utility tradeoff is impossible as long as nodes use shortest-path routing. Since there is a monetary cost associated with taking longer paths, most users are likely to default to shortest-path routing. Nonetheless, some users do care about privacy and may be willing to pay for it [3, 5]. The next section explores various techniques for breaking the diagonal bound, and the costs associated with doing so.

4 BREAKING THE DIAGONAL BARRIER

The goal of this section is to break the diagonal barrier imposed by Theorem 3.2 by relaxing the assumptions on which it is based. We consider two relaxations: one related to adding uncertainty to the candidate endpoint set, and the other related to adding uncertainty to the set of candidate paths. More precisely, Theorem 3.2 makes two main assumptions: (i) utility $U(\mathbb{D})$ is computed as a minimum over all network edges, as in the definition (2.2), and (ii) all transactions are routed using a shortest path between the source and destination. We will relax the first assumption to introduce endpoint uncertainty, and the second to introduce path uncertainty.

Assumption (i): Definition (2.2) of utility may not be appropriate when the PCN includes endpoint nodes with degree one, or clients that connect to “gateway” routers. This could happen, for example, if PCNs evolve so that merchants run the majority of router nodes, which maintain several well-funded channels, and end users connect to merchants only for their own transactions, i.e., without participating in transaction relaying. As an extreme example, consider a star network, which is a tree of depth one. Any routing of a transaction requires at most two edges, whose balances are already known to the nodes directly involved in the transaction, i.e., the sender and the receiver. Because the sender and receiver already know the balances on their adjacent edges, they could transmit this information out of band, so hiding the balance of any edge does not decrease success rate, but provides perfect privacy against an external observer. In Section 4.1, we show how to improve the privacy-utility tradeoff by allowing the source and destination to exchange their adjacent true balances prior to transacting.

Assumption (ii): The second assumption might not hold if users are willing to route transactions over paths longer than the shortest path(s). At the cost of incurring more fees, such longer routing can intuitively achieve better privacy-utility tradeoff. Although the gains are difficult to quantify in general, we precisely quantify them for a special network topology in Section 4.2.

4.1 Endpoint Uncertainty

In real-world PCNs, users know the true balances (or weights) on their directly adjacent channels (or edges). For example, when a user Alice tries to transact with neighboring user Bob, Alice and Bob already know each other’s true balances. Therefore, for any direct transaction among neighbors, success rate is not sacrificed even if the balances are kept private. In an extension of this idea, consider a PCN model with *users* and *servers*; users make transactions among themselves, whereas servers relay them. Servers are connected in a

network structure $(\mathcal{V}_S, \mathcal{E}_S)$, whereas each user node is connected to one server node. Let $\mathcal{V}_U, \mathcal{E}_U$ denote the set of user nodes and user-server channels, respectively. Then there exist functions $J : \mathcal{V}_U \rightarrow \mathcal{V}_S$ and $K : \mathcal{V}_U \rightarrow \mathcal{E}_U$, where for a user node $v \in \mathcal{V}_U$, $J(v)$ is the server to which v is connected, and $K(v)$ is its unique incident channel, which connects v and $J(v)$. Furthermore, let $(n_S, n_U) = (|\mathcal{V}_S|, |\mathcal{V}_U|)$. The public balances on the user-server channels are never updated, while those on the inter-server channels are updated with a privatizing noise mechanism of our choice.

Under the following assumption that the set \mathcal{P} of available paths are not too restricted, we show that just privatizing the inter-server channels is sufficient to achieve improved privacy-utility tradeoff.

ASSUMPTION 1. For any oriented path $P \in \mathcal{P}$ from x to y ,

- if $x \notin \mathcal{V}_S$, then $P - \{(x, J(x))\} \in \mathcal{P}$;
- if $x \in \mathcal{V}_S$, then $\forall v : J(v) = x$, we have $\{(v, x)\} \cup P \in \mathcal{P}$;
- if $y \notin \mathcal{V}_S$, then $P - \{(J(y), y)\} \in \mathcal{P}$;
- if $y \in \mathcal{V}_S$, then $\forall v : J(v) = y$, we have $\{(y, v)\} \cup P \in \mathcal{P}$.

PROPOSITION 4.1. Suppose we have a user-server network $(\mathcal{V}_S \cup \mathcal{V}_U, \mathcal{E}_S \cup \mathcal{E}_U)$, and the set \mathcal{P} of available paths satisfy Assumption 1, the server sub-network $(\mathcal{V}_S, \mathcal{E}_S)$ is reachable under \mathcal{P} , and all the transactions are routed via the shortest paths. When the channels on the server network $(\mathcal{V}_S, \mathcal{E}_S)$ have balances governed by the all-or-nothing noise mechanism \mathbb{D}_N with utility $U(\mathbb{D}_N) = \alpha$, and the channels on the user network $(\mathcal{V}_U, \mathcal{E}_U)$ are completely hidden, the privacy metric $\Pi(\mathbb{D}_N)$ is

$$\Pi(\mathbb{D}_N) = \left(1 - \frac{2}{n_S + n_U}\right)(1 - \alpha) + \frac{\mu}{\mu + 1}\alpha, \quad (4.1)$$

where μ is a lower bound on the number of users attached to any server node.

Compared with all-or-nothing noise on a full PCN (Theorem 3.6), the privacy level of the user-server model is higher by $\mu U(\mathbb{D}) / (1 + \mu)$. Figure 7, left panel, plots the gains achievable from Theorem 4.1 under all-or-nothing noise. As the number of users per server increases, we get improved tradeoffs, eventually achieving maximum privacy with no utility loss in the limit as $\mu, n_S, n_U \rightarrow \infty$. Intuitively, the adversary cannot distinguish between sources or destinations connected to the first and last server nodes. Since the adjacent user nodes as well as the last server node can all be the real destination of money flow, the adversary's best strategy is to guess uniformly at random. Hence the gain in privacy comes from the increased uncertainty at the end nodes, which does not sacrifice the success rate of routing transactions. This observation can be generalized to each user having multiple connections to servers, as long as the users do not relay transactions. Moreover, preliminary evidence suggests that user-server models may naturally emerge in practice; thus far, we have seen the emergence of routing hubs on the Lightning network, complemented by many users with few channels (Figure 15).

4.1.1 *Proof of Proposition 4.1.* For path $P \in \mathcal{P}$, let \bar{P} denote P excluding the user-server channels, if they exist. If the all-or-nothing noise \mathbb{D}_N selects "nothing", then the adversary sees no update. Otherwise, the adversary will see \bar{P} instead of P in our original model

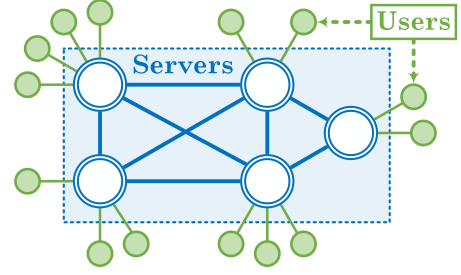


Figure 5: The user-server model consists of server nodes that route transactions, and user nodes who make transactions, but do not relay other nodes' transactions.

analyzed in Section 3. By definition of privacy,

$$\begin{aligned} \Pi(\mathbb{D}_N) &= 1 - \sup_{\mathbb{A}} \min_P \{ \mathbb{A}[\partial P|\bar{P}]\alpha + \mathbb{A}[\partial P|\emptyset](1 - \alpha) \} \\ &= 1 - \sup_{\mathbb{A}[\cdot|\bar{P}], \mathbb{A}[\cdot|\emptyset]} \min_P \{ \mathbb{A}[\partial P|\bar{P}]\alpha + \mathbb{A}[\partial P|\emptyset](1 - \alpha) \} \\ &\stackrel{(*)}{\leq} 1 - \sup_{\mathbb{A}[\cdot|\bar{P}], \mathbb{A}[\cdot|\emptyset]} \left[\alpha \min_P \mathbb{A}[\partial P|\bar{P}] + (1 - \alpha) \min_{P'} \mathbb{A}[\partial P'|\emptyset] \right] \\ &= 1 - \alpha \sup_{\mathbb{A}[\cdot|\bar{P}]} \min_P \mathbb{A}[\partial P|\bar{P}] - (1 - \alpha) \sup_{\mathbb{A}[\cdot|\emptyset]} \min_{P'} \mathbb{A}[\partial P'|\emptyset], \end{aligned}$$

where the last line follows because $\mathbb{A}[\cdot|\bar{P}]$ and $\mathbb{A}[\cdot|\emptyset]$ are independent. Because the network is reachable, we may apply Lemma 3.5 and obtain

$$\sup_{\mathbb{A}} \min_{P'} \mathbb{A}[\partial P'|\emptyset] = \frac{2}{n_S + n_U},$$

where the adversary reaches the supremum by choosing each node with equal probability when it sees no balance update.

Now we compute $\sup_{\mathbb{A}} \min_P \mathbb{A}[\partial P|\bar{P}]$. Since \bar{P} must be a path between server nodes, we let x, y denote them and define two sets

$$X \triangleq \{x\} \cup \{v \in \mathcal{V}_U | J(v) = x\}, \quad Y \triangleq \{y\} \cup \{v \in \mathcal{V}_U | J(v) = y\}.$$

If $x = y$, then the transaction only goes through user-server channels and $\bar{P} = \emptyset$. The adversary will see no update regardless of utility α , so random guessing with equal probability is the best adversarial strategy. Now we assume $x \neq y$, and immediately $X \cap Y = \emptyset$. The two endpoints of P must lie in each of X and Y . Because $\mathbb{A}[\cdot|\bar{P}]$ is a probability distribution, for any \mathbb{A} there exists $u \in X$ and $v \in Y$, where

$$\mathbb{A}[u|\bar{P}] + \mathbb{A}[v|\bar{P}] \leq \max \left\{ \frac{1}{|X|}, \frac{1}{|Y|} \right\}.$$

By the properties of a user-server model, there exists a path P_u containing \bar{P} , and connecting u and v . Hence, we have

$$\sup_{\mathbb{A}} \min_P \mathbb{A}[\partial P'|\bar{P}] \leq \sup_{\mathbb{A}} \mathbb{A}[\partial P_u|\bar{P}] \leq \max \left\{ \frac{1}{|X|}, \frac{1}{|Y|} \right\} \leq \frac{1}{\mu + 1}. \quad (4.2)$$

Recall that \mathbb{A}_S was previously defined as $\mathbb{A}_S[v|Q] = 1/(n_S + n_U)$ for all $v \in \mathcal{V}$, if $Q = \emptyset$. We supplement this definition by defining it also in the case $Q \neq \emptyset$. Recall that all-or-nothing noise \mathbb{D}_N is being used, and Q must be a shortest path on the server network $(\mathcal{V}_S, \mathcal{E}_S)$ from x' to y' . Similar to X and Y , we use the following

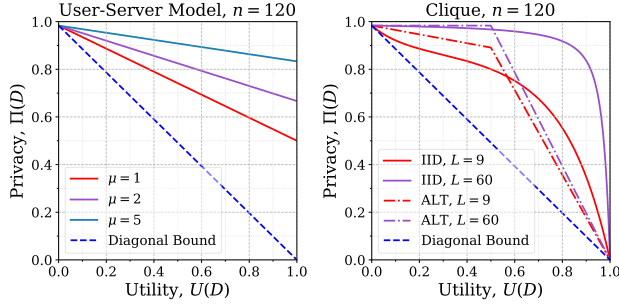


Figure 7: Exploiting the structures of the networks, we can design mechanisms that overcome the diagonal bound of Theorem 3.2 (shown in blue dashed line). Under the user-server model, we exploit endpoint uncertainty and under the clique model, we exploit path uncertainty.

order of magnitude. Hence, using longer paths appears to have diminishing returns for alternating noise.

Another natural mechanism which requires less coordination among the nodes in a path is the *i.i.d. noise mechanism*.

Definition 4.5. The **i.i.d. noise mechanism** \mathbb{D}_I updates the balance of each edge independently with constant probability $U(\mathbb{D}_I)$. Mathematically, for a path P with length L ,

$$\mathbb{D}_I[Q|P] = [U(\mathbb{D}_I)]^{|Q|} [1 - U(\mathbb{D}_I)]^{L-|Q|}, \quad \forall Q \subseteq P.$$

This noise mechanism enjoys similar privacy gains as the alternating mechanism due to path uncertainty. The main difference is that the number of candidate endpoints is now a random variable. We characterize the utility/privacy tradeoff precisely below.

THEOREM 4.6. *Suppose $(\mathcal{V}, \mathcal{E})$ is a complete graph and \mathcal{P} is the set of all simple paths of fixed length L . The privacy $\Pi(\mathbb{D}_I)$ of i.i.d. noise mechanism \mathbb{D}_I on a complete graph is lower bounded by*

$$\Pi(\mathbb{D}_I) \geq 1 - \frac{2(1-\alpha)^L}{n} - \frac{2}{(L+1)(1-\alpha)} \left[1 - \alpha^{L+1} - (1-\alpha)^{L+1} \right], \quad (4.6)$$

where $\alpha = U(\mathbb{D}_I)$ is the utility.

Figure 7 (right) plots the achievable bounds of Theorems 4.4 and 4.6, illustrating that neither scheme strictly dominates the other. However, i.i.d. noise has a larger jump in performance as we move from paths of length $L = 9$ to $L = 60$. Due to space constraints, the proofs of Theorems 4.4 and 4.6 can be found in Appendix A.

Takeaway Message. In this section, we show that the diagonal bound can be broken through two techniques: adding endpoint uncertainty and adding path uncertainty. Our exploration of path uncertainty in particular is limited to complete graphs due to the computational complexity of evaluating privacy metric (2.1) on general graphs. Still, we conjecture that similar intuitions can be applied to more complex, structured graphs; for instance, we relied on both the symmetry and the well-connected nature of complete graphs in our analysis; some circulant graphs exhibit similar properties. Hence, a takeaway message is that if one has the ability to choose a network structure, noise mechanism, and routing policy,

it is possible to achieve an improved privacy-utility tradeoff. This comes at the cost of higher transaction fees due to the choice of routing through longer paths. On the other hand, the user-server model arises organically in current payment channels, and is compatible with cost-effective, shortest-path routing.

5 SIMULATIONS

Success rate is one of the key metrics that system designers want to maximize; however, due to the complexity of theoretically quantifying success rate, we have analyzed a related quantity (utility) in this work. In this section, we empirically investigate the tradeoff between success rate and privacy in simulation. The purpose of these simulations is twofold: first, we want to understand how the privacy-utility tradeoffs analyzed earlier translate into a privacy-success rate tradeoff. Second, we want to understand the effects of network properties not captured by our analysis, such as graph topology, transaction workload, and initial capacity distribution.

Our simulator models the sequential processing of a *workload*: a sequence of *transactions*, or tuples consisting of a sender, a receiver, and a transaction value. To match behavior in real deployments, each transaction is routed using shortest-path routing on the weighted graph, where routes are determined from public balances. A transaction fails if either no route can be found, or if the user tries a route whose true balances are insufficient to support the transaction. When a transaction fails, we do not allow retries. In line with theorems 3.2 and 3.6, we use the all-or-nothing noise scheme $\mathbb{D} = \mathbb{D}_N$ with optimal privacy-utility tradeoff (3.4). Hence, after each transaction, we update all path balances with probability $U(\mathbb{D}_N)$, drawn independently for each transaction. We compute success rate by counting the fraction of successfully-processed transactions. Our theoretical results suggest that one can trade some privacy for an equal amount of utility. The question is, when we sacrifice one unit of privacy for one of utility, does this translate into a gain of more than one unit of success rate?

Privacy-success rate curves depend on many factors, including the choice of network, workload, noise mechanism, and initial balance/capacity allocations. For each parameter setting, we generated 100 sets of networks and/or workloads in advance and ran each workload on its corresponding network, with the appropriate noise mechanism. We plot the mean success rate and standard error bars.

5.1 Network Structure

Our first set of experiments considers the effects of network structure on performance. We consider both synthetic and real network structures. For real network topologies, we use a snapshot of the **Lightning Network** and its channel capacities measured on December 28, 2018. The network consists of 2,266 nodes and 15,392 channels, while channel capacities vary from 1,100 to 16,777,216 = 2^{24} satoshis (1 satoshi = 10^{-8} Bitcoin). For synthetic structures, we use Erdős-Rényi graph with different sizes and densities, where for a PCN with n nodes and m channels, density is defined as $2m/[n(n-1)]$. We fixed the synthetic network sizes to 2,266 to match the Lightning Network dataset. We evaluated three densities: **(a) low density**: $\rho_L(2266)$, which equals $\log 2266/2266 \approx 3.41 \times 10^{-3}$. This is the minimum density needed to keep the network connected with high probability. **(b) Lightning Network density**:

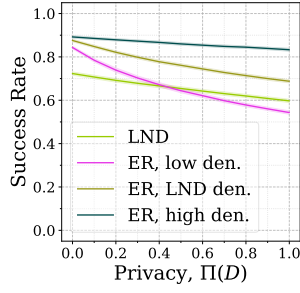


Figure 8: Success rate-privacy curves on different network topologies. Success rate is the fraction of successful transactions out of total 3,000.

$\rho_{\text{LND}}(2266) \approx 6.00 \times 10^{-3}$. This is the density measured from the LND dataset, and is calculated given that the number of channels is 15,392. **(c) high density:** $\rho_{\text{H}}(2266) = 5\rho_{\text{L}}(2266) \approx 17.0 \times 10^{-3}$. We also explore the effects of varying network size in Appendix B.

Initial balances and transaction workloads are unavailable on the Lightning Network because it operates in the high privacy regime. Hence, we chose initial channel capacities according to the observed capacity distribution, then uniformly allocated the balances on both ends of each channel. For the transaction workload, there is again no canonical dataset available, so we uniformly and independently drew 2 nodes as the sender and receiver of each transaction, with transaction values independently following a Pareto distribution $\Psi(1.16, 1000)$. We chose a Pareto distribution to make the transaction value distribution heavy-tailed, and selected parameters corresponding to the Pareto principle. $\Psi(\beta, v_m)$ has CDF

$$F(v) = \left[1 - \left[\frac{v_m(\beta - 1)}{\beta v} \right]^\beta \right] \cdot \mathbb{I} \left[v \geq \frac{v_m(\beta - 1)}{\beta} \right].$$

Random variable $V \sim \Psi(\beta, v_m)$ has mean $\mathbb{E}[V] = v_m$. So our expected transaction value and channel capacities equal 1,000 sat.

The privacy-success rate tradeoff curves with error bars are shown in Figure 8. The width of error bars suggests a low standard error. Notice three trends: First, as privacy level increases, success rate decreases. This makes intuitive sense, as having less accurate information about channel balances causes more transactions to fail due to false positives, where the user believes a path has enough balance from the public balances, but in reality it does not. However, we will see in Section 5.2 that this is not always the case. Second, as density decreases among the ER graphs, success rate appears to drop. This follows because lower-density graphs have fewer channels; since we draw each channel capacity i.i.d. from the same distribution, the total funding of the network is lower in low-density networks. Our third observation is the main takeaway message of this plot: **for the same density and number of nodes, the LND topology has a strictly lower success rate than the ER graph.** This appears to follow from the highly asymmetric nature of the LND graph (Figure 15). The LND network has several very high-degree nodes, with the remaining nodes generally connecting to only a few other nodes. This hub-and-spokes-like topology appears

to exacerbate channel imbalance; if a few key channels become imbalanced, it affects the success rates of the whole network. This illustrates the value of path diversity in PCNs.

Tradeoffs. Recall that one of our main goals was to understand if the one-to-one tradeoff of privacy for utility extends to success rate. Figure 8 suggests that this is not the case. For example, on the LND curve in Figure 8, if we start at today’s operating point of perfect privacy, one must decrease privacy by 0.8 to gain 0.1 units of success rate. More generally, the curves in these figures are convex with low curvature; sacrificing some amount of privacy gives disproportionately small gains in success rate. This suggests that system designers must sacrifice significant amounts of privacy to achieve meaningful improvements in success rate.

5.2 Workload size

We next investigate the role of workload size by varying the number of transactions in our workload. Figure 9 shows the average success rate as a function of privacy as we process from 70 to 30,000 transactions. Both subfigures have 100 nodes, and the ER graph has a density of $\log(100)/100$. More precisely, this experiment revealed two unexpected phenomena: (1) for all privacy levels (including zero), success rate decreases as we process more transactions. It is not obvious *a priori* why this should happen, as transactions are generated uniformly at random between nodes; on average, transaction flows should be balanced. (2) Success rate is not always monotonically decreasing in the privacy parameter. As we process higher numbers of transactions, we observe a minimum in the success rate-privacy curve at high (< 1) privacy levels. We explore each of these phenomena separately.

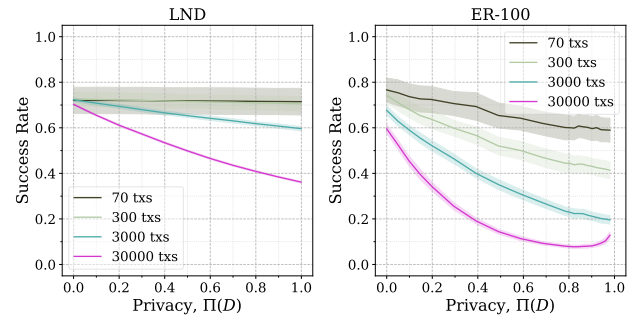


Figure 9: Transaction workload size vs success rate.

Non-monotonicity of success rate. To understand this phenomenon more carefully, we ran the same experiment as in Figure 9 on a single-edge PCN, over 100 experiments. Figure 10 plots the real channel balances vs the observed ones for this edge as the number of transactions T grows. Each row represents a different utility level; utility 0 corresponds to perfect privacy. Notice that over time, the edge becomes *deadlocked*. In other words, although the public balance appears to be concentrated on one side of the channel, the true balance is concentrated on the other. If this imbalance is extreme enough, it prevents any transactions from passing through the channel in either direction. This explains the non-monotonicity

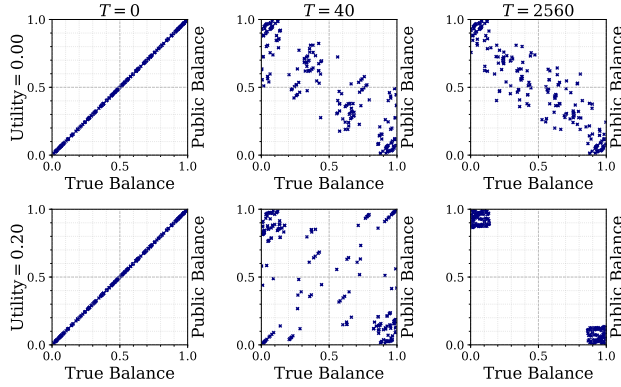


Figure 10: True vs. public balance for a single-edge PCN.

of Figure 9; at high privacy levels, not only are deadlocks likely to form, but the transactions that do pass are less likely to reverse the deadlock by revealing the true channel balances, since the probability of updating channel balances is low. Hence, once a channel is deadlocked, it can remain so for a long time. In contrast, at perfect privacy, we observe relatively fewer deadlocks because public channel balances remain forever at their initial values. Notice that in such a scenario, a deadlock can only form if a channel *starts* in an imbalanced state (e.g., 100 tokens on one side, 900 on the other), but eventually moves most of its balance to the other side. This event is relatively rare because our channel balances are initialized uniformly in these experiments.

These deadlocks suggest that sacrificing a little privacy can actually *hurt* average success rate in the long term. Hence system designers should be wary of deploying a noise mechanism that sacrifices only a little privacy; not only are the gains modest in theory, they can actually be negative in practice, unless system designers deal with deadlocks.

Declining success rate over time. The declining success rates are partially due to the previously-described deadlocks. However, we observe the phenomenon even at zero privacy, when deadlocks cannot happen. The reason may be related to the formation of *routing bottlenecks*. Suppose a node v receives many transactions until all of v 's neighboring channels are imbalanced, with most of the balance on v 's side of the channel. In such a scenario, nobody can route through v : funds cannot reach v , so it cannot relay money. Under randomized transaction workloads like ours, such bottlenecks are theoretically recurrent; in practice, they can also occur if some nodes are popular money recipients (e.g., merchants). The only way to break a bottleneck is for the bottlenecked node(s) to send their own transactions out of the isolated zone. In a large network, the likelihood of this happening for a uniform workload is small. Hence, the system may be bottlenecked for a long time.

5.3 Transaction Value

In the previous experimental settings, the value of every transaction followed a Pareto distribution $\Psi(1.16, 1000)$. To study the curves for different transaction value distributions, we first selected two typical network structures: Lightning Network and

Erdős-Rényi network with the same size and density. We also fixed the size of the workload to 3,000 transactions. We considered two properties of transaction values: distribution type and expectation. The distribution types include the uniform distribution from 0 to twice the expected value, and 3 different Pareto distributions with $\beta = 1.1, 1.16, 1.25$. Their PDFs are plotted in Figure 14 (Appendix B). Figure 11 illustrates the privacy-success rate tradeoffs for each of these experimental settings. Here, the “unbalanced” curve in the top row refers to our approach for generating the endpoints of transactions; instead of choosing the source and destination uniformly, we assign users a weight of 1 with probability 0.8 and 16 with probability 0.2. When generating transactions, we sample endpoints with probability proportional to their weights. On average, 20% of the users hold 80% of the weight; this models the imbalance observed in real financial transactions. These plots show that when the mean transaction value increases, the success rate decreases. This is because we are keeping the capacity distribution fixed, so larger transactions are more likely to fail. Similarly, using increasingly heavy-tailed Pareto transactions (smaller β) causes the minimum transaction value to decrease, which increases the success rate. Although these plots illustrate some trends related to transaction value distribution, the main takeaway is the fact that for a variety of transaction value distributions, the slope of the privacy-success rate curves is shallow. This implies that **one cannot trade small losses in privacy for large gains in success rate, or vice versa**.

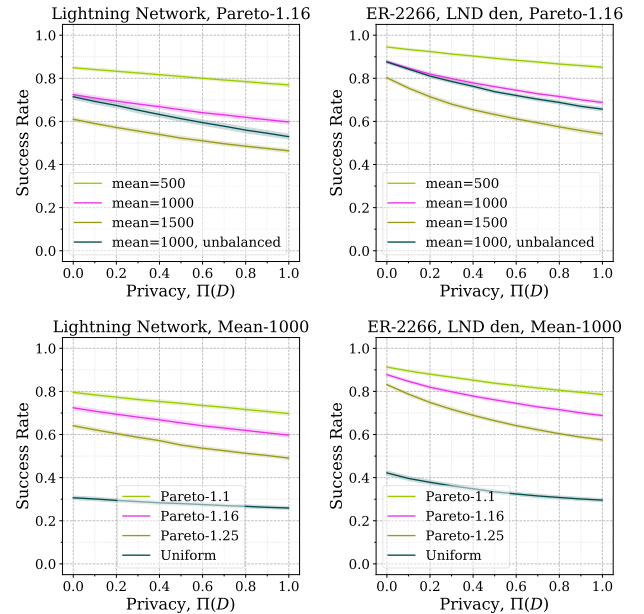


Figure 11: Success rate-privacy tradeoffs for different transaction value distributions. The left column considers Pareto-distributed transactions of different means; the right column considers different distributions with the same mean.

6 RELATED WORK

PCNs have received substantial attention recently from the academic community. Papers in this space typically focus either on privacy or on utility. To our knowledge, our work is the first to explicitly quantify tradeoffs between privacy and utility in PCNs.

On the utility front, papers have primarily focused on improving the success rates of PCNs. This is typically achieved through new routing mechanisms, which exploit ideas from the networking literature, such as packet-switched routing, congestion control, and/or flow control [10, 24]. Our work differs from these papers in that it assumes source-routed transactions. This decision is made primarily for analytical tractability; understanding the effects of packet-switched routing is an important direction for future work. Other recent utility work has instead focused on related but orthogonal issues, such as preventing deadlocks in PCNs [19, 28] and rebalancing depleted channels [17].

On the privacy front, several papers have explored mechanisms for privacy-preserving routing, both in the context of PCNs [18, 23] and in general communication networks [8, 9, 14, 20]. Indeed, onion routing is used in today's Lightning network [9]. Some of the PCN-specific mechanisms were later shown to exhibit worse utility than the Lightning network [24], though their privacy guarantees are stronger. There are two key differences between the prior literature on privacy-preserving PCN routing and our work. First, our adversary is a passive observer of the information publicly released to all participants, whereas prior work like [9, 14, 18, 23] considers a corrupt relay node that is trying to learn the destination of a transaction. Prior work by Malavolta *et al.* [19] has studied the notion of *passive value privacy*, or hiding the amount of a transaction to a passive external observer; they also study *active relationship anonymity*, which aims to hide the participants of a transaction to an active router. Our model is a combination of these; it considers a passive observer that wants to infer the endpoints of a transaction; in our setting, hiding transaction value would be easier than hiding endpoints. Hence, our adversarial model is weaker than prior work in the sense that it sees less information than a router node, but stronger in the sense that encrypting the destination of a transaction does not solve the problem. Note that our results are negative, so with a stronger active adversary, even worse tradeoffs could emerge. Second, our privacy problem is fundamentally different from that addressed in prior work. Because all network participants must be able to route transactions, encrypting transaction balances is not a viable solution; statistical noise therefore is a more natural solution. The most closely related work to ours ([19]) explicitly does not consider the problem of path selection, focusing instead on how to execute transactions once a path is selected.

Orthogonal to the privacy preserving PCN protocols studied in this paper, there are privacy threats in blockchain P2P networking protocols. This was demonstrated in [6] where researchers successfully linked 30% of Bitcoin users' public keys to their IP addresses. Such de-anonymization reveals sensitive financial information about the owners of the cryptocurrency. The attack exploits vulnerabilities in the Bitcoin P2P networking stack, whose privacy implications are poorly understood. A new protocol for broadcasting transactions [7] is shown to achieve near optimal anonymity guarantees, at minimal cost to network utility.

Notice that differential privacy (a common statistical privacy metric) is difficult to implement in our setting [11]. For example, consider providing ϵ -local differential privacy on the source of a transaction [16]. This would require that for any observed path trace Q and any pair of candidate source nodes $u, v \in \mathcal{V}$, it must hold that $\mathbb{P}[Q|s(P) = v] \leq e^\epsilon \mathbb{P}[Q|s(P) = u]$. To achieve this condition, we would need to add noise to edges that are not involved in the transaction itself; this adds significant overhead, both in terms of implementation and in terms of added noise. Like differential privacy, our metric is worst-case; however, it does not require hiding the transaction participants among all nodes in the graph.

7 DISCUSSION

In this paper, we have shown that for an important class of routing mechanisms (shortest-path routing), it is not possible to obtain a good privacy-utility tradeoff by releasing noisy channel balances in PCNs. The diagonal bound places an upper limit on the privacy-utility tradeoff obtainable in practice, and it is tight for general graph topologies. Our theoretical results are backed by simulations, which show that even if one considers a more complex end utility metric (i.e. success rate), the tradeoff does not improve; in fact, it appears to worsen in some cases. For example, we observe a new deadlocking phenomenon, by which channels end up severely imbalanced in one direction, while the public balances are severely imbalanced in the other. These deadlocks are impossible to revert for a transaction distribution with a minimum transaction value, such as the Pareto distributions used in our simulations. In practice, the situation may not be so dire; small transactions may be able to prevent the formation of total deadlocks. Another key observation is that our privacy analysis considers a passive adversary. An active adversary, which is stronger, could cause these tradeoffs to degrade.

Our findings suggest that network operators may not want to introduce noisy balance reporting mechanisms to trade off privacy for utility. Starting from today's operating point of perfect privacy, a network would need to give up almost all privacy to obtain substantial gains in success rate. As long as users use shortest-path routing, network operators may be better off choosing one extreme operating point or the other: perfect utility or perfect privacy.

Despite these pessimistic conclusions, our analysis does not close the book on this issue. It may be possible to obtain a more promising tradeoff by modeling the effects of concurrent transactions and packet-switched routing, where transactions are split into smaller units and sent over different paths. Packet-switched routing can cause transactions to flow over a much larger fraction of network edges per transaction. This may have a similar effect to the long-path analysis in Section 4.2 of confusing the adversary regarding the endpoints of the transaction. Analyzing such routing mechanisms is an important and interesting question for future work.

ACKNOWLEDGMENTS

This work is supported by NSF with grant number CIF-1705007, by ARO with grant number ARO-W911NF-17-S-0002, and by Input Output Hong Kong.

REFERENCES

- [1] Lightning network daemon. <https://github.com/lightningnetwork/lnd>.
- [2] Raiden network. <https://raiden.network/>.

- [3] Alessandro Acquisti, Leslie K John, and George Loewenstein. What is privacy worth? *The Journal of Legal Studies*, 42(2):249–274, 2013.
- [4] Billy Bambrough. Bitcoin just crossed a huge adoption milestone. *Forbes*, 2019.
- [5] Alastair R Beresford, Dorothea Kübler, and Sören Preibusch. Unwillingness to pay for privacy: A field experiment. *Economics letters*, 117(1):25–27, 2012.
- [6] Alex Biryukov, Dmitry Khovratovich, and Ivan Pustogarov. Deanonimisation of clients in bitcoin p2p network. In *Proceedings of the 2014 ACM SIGSAC Conference on Computer and Communications Security*, pages 15–29. ACM, 2014.
- [7] Shaileshh Bojja Venkatakrishnan, Giulia Fanti, and Pramod Viswanath. Dandelion: Redesigning the bitcoin network for anonymity. *Proceedings of the ACM on Measurement and Analysis of Computing Systems*, 1(1):22, 2017.
- [8] Srdjan Capkun, Jean-Pierre Hubaux, and Markus Jakobsson. Secure and privacy-preserving communication in hybrid ad hoc networks. Technical report, 2004.
- [9] Roger Dingledine, Nick Mathewson, and Paul Syverson. Tor: The second-generation onion router. Technical report, Naval Research Lab Washington DC, 2004.
- [10] Mo Dong, Qingkai Liang, Xiaozhou Li, and Junda Liu. Celer network: Bring internet scale to every blockchain. *arXiv preprint arXiv:1810.00037*, 2018.
- [11] Cynthia Dwork. Differential privacy. *Encyclopedia of Cryptography and Security*, pages 338–340, 2011.
- [12] Ittay Eyal, Adem Efe Gencer, Emin Gün Sirer, and Robbert Van Renesse. Bitcoin-ing: A scalable blockchain protocol. In *13th {USENIX} Symposium on Networked Systems Design and Implementation ({NSDI} 16)*, pages 45–59, 2016.
- [13] David Floyd. Lightning network: What is it and can it solve bitcoin's scaling problem? *Investopedia*, March 2018.
- [14] Michael J Freedman and Robert Morris. Tarzan: A peer-to-peer anonymizing network layer. In *Proceedings of the 9th ACM conference on Computer and communications security*, pages 193–206. ACM, 2002.
- [15] Julio Gil-Pulgar. Atomic Multi-Path to help Bitcoin become a formidable payment instrument. *Bitcoinist*, February 2018.
- [16] Peter Kairouz, Sewoong Oh, and Pramod Viswanath. Extremal mechanisms for local differential privacy. In *Advances in neural information processing systems*, pages 2879–2887, 2014.
- [17] Rami Khalil and Arthur Gervais. Revive: Rebalancing off-blockchain payment networks. In *Proceedings of the 2017 ACM SIGSAC Conference on Computer and Communications Security*, pages 439–453. ACM, 2017.
- [18] Giulio Malavolta, Pedro Moreno-Sanchez, Aniket Kate, and Matteo Maffei. Silentspeakers: Enforcing security and privacy in decentralized credit networks. In *NDSS*, 2017.
- [19] Giulio Malavolta, Pedro Moreno-Sanchez, Aniket Kate, Matteo Maffei, and Srivatsan Ravi. Concurrency and privacy with payment-channel networks. In *Proceedings of the 2017 ACM SIGSAC Conference on Computer and Communications Security*, pages 455–471. ACM, 2017.
- [20] Animesh Nandi, Armen Aghasaryan, and Makram Bouzid. P3: A privacy preserving personalization middleware for recommendation-based services. In *Hot Topics in Privacy Enhancing Technologies Symposium*, 2011.
- [21] Dmytro Piatkivskiy and Mariusz Nowostawski. Split payments in payment networks. In *Data Privacy Management, Cryptocurrencies and Blockchain Technology*, pages 67–75. Springer, 2018.
- [22] Joseph Poon and Thaddeus Dryja. The bitcoin lightning network: Scalable off-chain instant payments, 2016.
- [23] Stefanie Roos, Pedro Moreno-Sanchez, Aniket Kate, and Ian Goldberg. Settling payments fast and private: Efficient decentralized routing for path-based transactions. *arXiv preprint arXiv:1709.05748*, 2017.
- [24] Vibhaalakshmi Sivaraman, Shaileshh Bojja Venkatakrishnan, Mohammad Alizadeh, Giulia Fanti, and Pramod Viswanath. Routing cryptocurrency with the spider network. *arXiv preprint arXiv:1809.05088*, 2018.
- [25] Kyle Torpey. Greg maxwell: Lightning network better than sidechains for scaling bitcoin. *Bitcoin Magazine*, April 2016.
- [26] Manny Trillo. Stress test prepares visanet for the most wonderful time of the year. <http://stress-test-prepares-visanet-for-the-most-wonderful-time-of-the-year/www.visa.com/blogarchives/us/2013/10/10/index.html>, 2013.
- [27] Neel Varshney. Lightning network has 1 percent success rate with transactions larger than \$200, controversial research says. *Hard Fork*, June 2018.
- [28] Shira Werman and Aviv Zohar. Avoiding deadlocks in payment channel networks. In *Data Privacy Management, Cryptocurrencies and Blockchain Technology*, pages 175–187. Springer, 2018.
- [29] Haifeng Yu, Ivica Nikolic, Ruomu Hou, and Prateek Saxena. Ohie: Blockchain scaling made simple. *arXiv preprint arXiv:1811.12628*, 2018.

APPENDIX

A PROOFS

We include proofs of the main results in this section.

A.1 Proof of Proposition 4.2

For path $P \in \mathcal{P}$, let \bar{P} denote P excluding the user-server channels, if they exist. Furthermore, let $Q = \{\bar{P} | P \in \mathcal{P}\}$. By definition of privacy,

$$\begin{aligned}
 & \Pi(\mathbb{D}_{\mathbf{N}}) \\
 &= 1 - \sup_{\mathbb{A}} \min_P \{ \mathbb{A}[\partial P | \bar{P}] \alpha + \mathbb{A}[\partial P | \emptyset] (1 - \alpha) \} \\
 &= 1 - \sup_{\mathbb{A}[\cdot | \emptyset], \mathbb{A}[\cdot | \emptyset]} \min_P \{ \mathbb{A}[\partial P | \bar{P}] \alpha + \mathbb{A}[\partial P | \emptyset] (1 - \alpha) \} \\
 &\stackrel{(*)}{\leq} 1 - \sup_{\mathbb{A}[\cdot | \emptyset], \mathbb{A}[\cdot | \emptyset]} \left[\alpha \min_P \mathbb{A}[\partial P | \bar{P}] + (1 - \alpha) \min_{P'} \mathbb{A}[\partial P' | \emptyset] \right] \\
 &= 1 - \alpha \sup_{\mathbb{A}[\cdot | \emptyset]} \min_P \mathbb{A}[\partial P | \bar{P}] - (1 - \alpha) \sup_{\mathbb{A}} \min_{P'} \mathbb{A}[\partial P' | \emptyset] \\
 &= 1 - \alpha \sup_{\mathbb{A}[\cdot | \emptyset]} \min_P \mathbb{A}[\partial P | \bar{P}] - \frac{2}{n} (1 - \alpha) \\
 &= 1 - \frac{2}{n} (1 - \alpha) - \alpha \min_{Q \in \mathcal{Q}} \sup_{\mathbb{A}[\cdot | Q]} \min_{P: P=Q} \mathbb{A}[\partial P | Q]. \quad (**)
 \end{aligned}$$

Note that by Lemma 3.5, $\sup_{\mathbb{A}} \min_{P'} \mathbb{A}[\partial P' | \emptyset] = 2/n$. Any adversarial strategy can achieve this supremum by guessing uniformly at random when seeing no updates.

For a server node v , we define its **cloud** C_v as below.

$$C_v = \{v\} \cup \{u \in \mathcal{V}_U | (u, v) \in \mathcal{E}_U\}.$$

Apparently, for all $v \in \mathcal{E}_S$, $|C_v| \geq \mu + 1$. Let $x, y \in \mathcal{V}_S$ where $x \neq y$. Since C_x and C_y are not disjoint anymore, we define

$$Z = C_x \cap C_y, X = C_x - Z, Y = C_y - Z.$$

Apparently, X, Y and Z are disjoint subsets with union $C_x \cup C_y$. In addition, $x \in X, y \in Y$. For now, we assume $|Z| \geq 2$, so that there exists a path whose both source and destination belong to Z .

Because the network is reachable, there exists a path Q on the server network $(\mathcal{V}_S, \mathcal{E}_S)$ connecting x and y . In addition, for any $x' \in C_x$ and $y' \in C_y$ where $x' \neq y'$, there exists a path P with endpoints x', y' , and containing Q . In this case, we have

$$\min_P \mathbb{A}_{\mathcal{S}}[\partial P | Q] = \min \{ p_X + p_Y, p_X + p_Z, p_Y + p_Z, 2p_Z \},$$

where for $W \in \{X, Y, Z\}$, $p_W \triangleq \min_{v \in W} \mathbb{A}_{\mathcal{S}}[v | Q]$. Now obviously, the best adversary $\mathbb{A}_{\mathcal{S}}$ satisfies for all $x' \in X, y' \in Y, z' \in Z$,

$$(\mathbb{A}_{\mathcal{S}}[x' | Q], \mathbb{A}_{\mathcal{S}}[y' | Q], \mathbb{A}_{\mathcal{S}}[z' | Q]) \equiv (p_X, p_Y, p_Z).$$

Hence, to obtain $\mathbb{A}_{\mathcal{S}}[\cdot | Q]$, we only need to determine the probabilities p_X, p_Y and p_Z by solving the following problem.

$$\begin{aligned}
 & \text{maximize} && \min \{ p_X + p_Y, p_Y + p_Z, p_Z + p_X, 2p_Z \} \\
 & \text{subject to} && |X| p_X + |Y| p_Y + |Z| p_Z = 1.
 \end{aligned} \quad (\text{A.1})$$

In order to deal with the minimum in the objective function, we discuss 4 cases.

Case 1: $p_Z \leq p_X, p_Y$. The objective function equals $2p_Z$, and

$$2p_Z \leq \frac{2(|X|p_X + |Y|p_Y + |Z|p_Z)}{|X| + |Y| + |Z|} = \frac{2}{|X| + |Y| + |Z|}.$$

By taking $p_X = p_Y = p_Z = 2/(|X| + |Y| + |Z|)$, the upper bound is attained. So in this case the maximum equals $2/(|X| + |Y| + |Z|)$.

Case 2: $p_Z \geq p_X, p_Y$. The objective function equals $p_X + p_Y$.

- If $||X| - |Y|| \leq |Z|$, we let $t = (|Y| - |X| + |Z|)/(2|Z|)$, which lies in $[0, 1]$. Then,

$$\begin{aligned} 1 &= |X|p_X + |Y|p_Y + |Z|p_Z \\ &\geq (|X| + t|Z|)p_X + [|Y| + (1-t)|Z|]p_Y \\ &= \frac{|X| + |Y| + |Z|}{2} (p_X + p_Y). \end{aligned}$$

So the maximum equals $2/(|X| + |Y| + |Z|)$, which is attained by taking $p_X = p_Y = p_Z = 2/(|X| + |Y| + |Z|)$.

- If $|Y| > |X| + |Z|$, we have

$$\begin{aligned} 1 &= |X|p_X + |Y|p_Y + |Z|p_Z \\ &\geq (|X| + |Z|)p_X + (|X| + |Z|)p_Y. \end{aligned}$$

The maximum equals $1/(|X| + |Z|)$, which is attained by taking $p_Y = 0$ and $p_X = p_Z = 1/(|X| + |Z|)$.

- If $|X| > |Y| + |Z|$, analogously, the maximum equals $1/(|Y| + |Z|)$ with maximizers $p_X = 0$ and $p_Y = p_Z = 1/(|Y| + |Z|)$.

To summarize, the maximum equals

$$\max \left\{ \frac{2}{|X| + |Y| + |Z|}, \frac{1}{|X| + |Z|}, \frac{1}{|Y| + |Z|} \right\}.$$

Case 3: $p_X \leq p_Z \leq p_Y$. The objective function equals $p_X + p_Z$.

- If $|X| > |Y| + |Z|$,

$$\begin{aligned} 1 &= |X|p_X + |Y|p_Y + |Z|p_Z \\ &\geq (|Y| + |Z|)p_X + |Y|p_Z + |Z|p_Z. \end{aligned}$$

This indicates maximum of $p_X + p_Z$ equals $1/(|Y| + |Z|)$ by picking $p_X = 0$ and $p_Y = p_Z = 1/(|Y| + |Z|)$.

- If $|X| \leq |Y| + |Z|$,

$$\begin{aligned} 1 &= |X|p_X + |Y|p_Y + |Z|p_Z \\ &\geq |X|p_X + (|Y| + |Z|)p_Z \\ &\geq \frac{|X| + |Y| + |Z|}{2} (p_X + p_Z). \end{aligned}$$

The last line is obtained by using Chebyshev's inequality, with conditions $|X| \leq |Y| + |Z|$ and $p_X \leq p_Z$. So the maximum of $p_X + p_Z$ equals $2/(|X| + |Y| + |Z|)$, which is attained at $p_X = p_Y = p_Z = 1/(|X| + |Y| + |Z|)$.

To summarize, the maximum equals

$$\max \left\{ \frac{2}{|X| + |Y| + |Z|}, \frac{1}{|Y| + |Z|} \right\}.$$

Case 4: $p_Y \leq p_Z \leq p_X$. Analogously, the maximum equals

$$\max \left\{ \frac{2}{|X| + |Y| + |Z|}, \frac{1}{|X| + |Z|} \right\}.$$

In general, the maximum may be simply expressed as below.

$$\sup_{\mathbb{A}[\cdot|Q]} \min_P \mathbb{A}[\partial P|Q] = \max \left\{ \frac{2}{|X| + |Y| + |Z|}, \frac{1}{|X| + |Z|}, \frac{1}{|Y| + |Z|} \right\}. \quad (\text{A.2})$$

To attain it, the optimal adversarial strategy $\mathbb{A}_{\mathfrak{S}}$ satisfies

- (1) if $||X| - |Y|| \leq |Z|$, then for all $v \in X \cup Y \cup Z$, $\mathbb{A}_{\mathfrak{S}}[v|Q] = 1/(|X| + |Y| + |Z|)$;
- (2) if $|X| > |Y| + |Z|$, then for all $x' \in X$ and $v \in Y \cup Z$, $\mathbb{A}_{\mathfrak{S}}[x'|Q] = 0$, $\mathbb{A}_{\mathfrak{S}}[v|Q] = 1/(|Y| + |Z|)$;
- (3) if $|Y| > |X| + |Z|$, then for all $y' \in Y$ and $v \in X \cup Z$, $\mathbb{A}_{\mathfrak{S}}[y'|Q] = 0$, $\mathbb{A}_{\mathfrak{S}}[v|Q] = 1/(|X| + |Z|)$.

It should be addressed that the above solution applies only when $|Z| \geq 2$. For the case $|Z| = 0$, we have $C_x \cap C_y = \emptyset$ equivalently. Proof of Proposition 4.1 has shown that the maximum value and the optimal strategy are actually compatible with (A.2). Hence, we only need to focus on the case $|Z| = 1$. The analysis begins to fork at the problem formulation, because there will be no path with both ends lying in set Z . So we need to modify (A.1) as followed.

$$\begin{aligned} &\text{maximize} \quad \min \{ p_X + p_Y, p_Y + p_Z, p_Z + p_X \} \\ &\text{subject to} \quad |X|p_X + |Y|p_Y + |Z|p_Z = 1. \end{aligned} \quad (\text{A.3})$$

After similar discussions, we can obtain the maximum

$$\max \left\{ \frac{2}{|X| + |Y| + |Z|}, \frac{1}{|X| + |Z|}, \frac{1}{|Y| + |Z|}, \frac{1}{|X| + |Y|} \right\}.$$

Because $|Z| = 1 \leq |X|, |Y|$, both (A.2) and $\mathbb{A}_{\mathfrak{S}}$ apply to this case. So we may regard them as a general solution, without respect to the value of $|Z|$. Recalling μ is the minimum number of user nodes connected to any server,

$$\begin{aligned} &\max \left\{ \frac{2}{|X| + |Y| + |Z|}, \frac{1}{|X| + |Z|}, \frac{1}{|Y| + |Z|} \right\} \\ &= \max \left\{ \frac{2}{|C_x \cup C_y|}, \frac{1}{|C_x|}, \frac{1}{|C_y|} \right\} \\ &\leq \max \left\{ \frac{2}{\mu + 2}, \frac{1}{\mu + 1}, \frac{1}{\mu + 1} \right\} = \frac{2}{\mu + 2}. \end{aligned}$$

Now we go back to privacy. It's easy to confirm that by substituting the supremum over \mathbb{A} with $\mathbb{A}_{\mathfrak{S}}$ at both sides of (*), it turns into an equality. Following (**),

$$\begin{aligned} \Pi(\mathbb{D}_{\mathbb{N}}) &= 1 - \frac{2}{n}(1 - \alpha) - \alpha \min_{Q \in \mathcal{Q}} \sup_{\mathbb{A}[\cdot|Q]} \min_{P: P=Q} \mathbb{A}[\partial P|Q] \\ &\geq 1 - \frac{2}{n}(1 - \alpha) - \alpha \min_{Q \in \mathcal{Q}} \frac{2}{\mu + 2} \\ &= \left(1 - \frac{2}{n} \right) (1 - \alpha) + \frac{\mu}{\mu + 2} \alpha. \end{aligned}$$

So the lower bound of privacy is justified. \square

A.2 Proof of Theorem 4.4

Let $\ell = \lfloor L/2 \rfloor$. Let \bar{P}_1 and \bar{P}_2 denote the "odd" group and "even" group of path P , respectively. We define

$$\begin{aligned} Q_i &\triangleq \{ \bar{P}_i | P \in \mathcal{P} \}, \quad i \in \{1, 2\}, \\ Z(v, Q) &\triangleq \{ \{ P | v \in \partial P, Q \in \{ \bar{P}_1, \bar{P}_2 \} \} \}. \end{aligned}$$

The method to analyse $Z(v, Q)$ depends on the parity of L .

Case 1: When $2 \mid L$, we have $\mathcal{Q}_1 = \mathcal{Q}_2$ (because the graph is complete). For convenience and consistency, we introduce some terminology that will be reused in the proof of Theorem 4.6. For any path trace Q of P , it consists of several disconnected segments, where each segment consists of one or more edges connected end to end (in the alternating noise scheme, each segment is only one edge). Each segment has two end nodes and zero or more intermediate nodes. We call the end nodes of a segment **gray nodes**, and the intermediate nodes are called **white nodes**. Again, in the alternating noise scheme, there are no white nodes; we will use white nodes in the proof of Theorem 4.6. The rest of the nodes in the network are called **black nodes**. Expressing these as sets, we let g_Q, w_Q and b_Q denote the sets of gray, white and black nodes given path trace Q . An example of segments and the aforementioned colors are shown in Figure 12.

For any path P under the alternating noise scheme, both \bar{P}_1 and \bar{P}_2 yield $L = 2\ell$ gray nodes and 1 black node. All nodes not on path P are always black nodes. If a gray node v is determined to be one endpoint of P , then its status as a source or destination is determined too. In that case, the other end must be a black node. So $Z(v, Q)$ equals the number of ways to pick this black node, multiplied by the number of ways to permute the remaining $\ell - 1$ segments. If a black node v is determined to be one end, it could be either a source or a destination. Then, $Z(v, Q)$ equals the number of ways to permute all ℓ segments, multiplied by 2, the number of ways to determine which end v is. That is,

$$Z(v, Q) = \begin{cases} (\ell - 1)!(n - 2\ell), & v \in g_Q; \\ 2\ell!, & v \in b_Q. \end{cases}$$

Case 2: When $2 \nmid L$, the case is different because for all $Q \in \mathcal{Q}_1$, Q has $\ell + 1$ edges, while for all $Q \in \mathcal{Q}_2$, Q has ℓ edges. As a result, $\mathcal{Q}_1 \cap \mathcal{Q}_2 = \emptyset$. For all $Q \in \mathcal{Q}_1$,

$$Z(v, Q) = \begin{cases} \ell!, & v \in g_Q; \\ 0, & v \in b_Q. \end{cases}$$

For all $Q \in \mathcal{Q}_2$,

$$Z(v, Q) = \begin{cases} 0, & v \in g_Q; \\ 2\ell!(n - 2\ell - 1), & v \in b_Q. \end{cases}$$

Define adversarial strategy \mathbb{A}_T as below. Note that $\mathbb{A}_T[v|\emptyset] = 1/n$ for all $v \in \mathcal{V}$. If balance updates of the entire path P are visible, \mathbb{A}_T directly picks an end node of it, so for all $P \in \mathcal{P}$, $\mathbb{A}_T[\partial P|P] = 1$.

(1) When $2 \mid L$,

$$\mathbb{A}_T[v|Q] = \begin{cases} \frac{\mathbb{I}[2L < n]}{L} + \frac{\mathbb{I}[2L = n]}{n}, & v \in g_Q; \\ \frac{\mathbb{I}[2L = n]}{n} + \frac{\mathbb{I}[2L > n]}{n - L}, & v \in b_Q. \end{cases}$$

(2) When $2 \nmid L$,

$$\mathbb{A}_T[v|Q] = \begin{cases} \frac{\mathbb{I}[Q \in \mathcal{Q}_1]}{L + 1}, & v \in g_Q; \\ \frac{\mathbb{I}[Q \in \mathcal{Q}_2]}{n - L + 1}, & v \in b_Q. \end{cases}$$

Based on calculations of $Z(v, Q)$, it's easy to confirm that

$$\mathbb{A}_T[\cdot|Q] \in \operatorname{argsup}_{\mathbb{A}[\cdot|Q]} \sum_{v \in \mathcal{V}} \mathbb{A}[v|Q]Z(v, Q), \quad \forall Q \in \mathcal{Q}_1 \cup \mathcal{Q}_2.$$

Now we analyse privacy based on the following discussions.

(1) When $\alpha \leq 1/2$,

$$\begin{aligned} & 1 - \Pi(\mathbb{D}_T) \\ &= \sup_{\mathbb{A}} \inf_{P \in \mathcal{P}} \{ \alpha \mathbb{A}[\partial P|\bar{P}_1] + \alpha \mathbb{A}[\partial P|\bar{P}_2] + (1 - 2\alpha) \mathbb{A}[\partial P|\emptyset] \} \\ &= \alpha \sup_{\mathbb{A}} \inf_{P \in \mathcal{P}} \{ \mathbb{A}[\partial P|\bar{P}_1] + \mathbb{A}[\partial P|\bar{P}_2] \} + \frac{2 - 4\alpha}{n} \quad (\text{A.4}) \\ &\stackrel{(\dagger)}{\leq} \frac{\alpha}{|\mathcal{P}|} \sup_{\mathbb{A}} \sum_{P \in \mathcal{P}} \{ \mathbb{A}[\partial P|\bar{P}_1] + \mathbb{A}[\partial P|\bar{P}_2] \} + \frac{2 - 4\alpha}{n} \\ &= \frac{\alpha}{|\mathcal{P}|} \sup_{\mathbb{A}} \sum_{Q \in \mathcal{Q}_1 \cup \mathcal{Q}_2} \sum_{v \in \mathcal{V}} \mathbb{A}[v|Q]Z(v, Q) + \frac{2 - 4\alpha}{n}. \end{aligned}$$

Note that (A.4) is obtained by Lemma 3.5, where $\mathbb{A}_T[\cdot|\emptyset]$ achieves the supremum. If we plug $\mathbb{A} = \mathbb{A}_T$ into both sides of (\dagger) by replacing the supremum, we get an equality. Hence, the left side supremum of (\dagger) is also achieved by \mathbb{A}_T . Therefore, we can calculate $\Pi(\mathbb{D}_T)$ as followed.

(a) When $2 \mid L$, let $P \in \mathcal{P}$ be arbitrary. In this case, both \bar{P}_1 and \bar{P}_2 have a gray end node and a black end node. Hence,

$$\begin{aligned} & \Pi(\mathbb{D}_T) \\ &= 1 - \alpha (\mathbb{A}_T[\partial P|\bar{P}_1] + \mathbb{A}_T[\partial P|\bar{P}_2]) - \frac{2 - 4\alpha}{n} \\ &= 1 + \frac{4\alpha - 2}{n} - 2\alpha \left(\frac{\mathbb{I}[2L < n]}{L} + 2 \frac{\mathbb{I}[2L = n]}{n} + \frac{\mathbb{I}[2L > n]}{n - L} \right) \\ &= 1 - \frac{2}{n} - \left(\frac{2}{\min\{L, n - L\}} - \frac{4}{n} \right) \alpha. \end{aligned}$$

(b) When $2 \nmid L$, let $P \in \mathcal{P}$ be arbitrary. Both end nodes are gray for \bar{P}_1 and black for \bar{P}_2 . Hence,

$$\begin{aligned} & \Pi(\mathbb{D}_T) = 1 - \alpha (\mathbb{A}_T[\partial P|\bar{P}_1] + \mathbb{A}_T[\partial P|\bar{P}_2]) - \frac{2 - 4\alpha}{n} \\ &= 1 + \frac{4\alpha - 2}{n} - \alpha \left(\frac{2\mathbb{I}[\bar{P}_1 \in \mathcal{Q}_1]}{L + 1} + \frac{2\mathbb{I}[\bar{P}_2 \in \mathcal{Q}_2]}{n - L + 1} \right) \\ &= 1 - \frac{2}{n} - \left(\frac{2}{L + 1} + \frac{2}{n - L + 1} - \frac{4}{n} \right) \alpha. \end{aligned}$$

(2) When $\alpha > 1/2$, with probability $(2\alpha - 1)$, public balances of P are updated. Hence,

$$\begin{aligned} & \Pi(\mathbb{D}_T) \\ &= 1 - \sup_{\mathbb{A}} \min_{P \in \mathcal{P}} \{ (1 - \alpha) \mathbb{A}_T[\partial P|\bar{P}_1] + (1 - \alpha) \mathbb{A}_T[\partial P|\bar{P}_2] + \\ & \quad (2\alpha - 1) \mathbb{A}_T[\partial P|P] \} \\ &= 1 - (2\alpha - 1) - (1 - \alpha) \sup_{\mathbb{A}} \min_{P \in \mathcal{P}} \{ \mathbb{A}_T[\partial P|\bar{P}_1] + \mathbb{A}_T[\partial P|\bar{P}_2] \}. \end{aligned}$$

Note that the supremum has been solved in the case $\alpha \leq 1/2$. So the results will be written below directly.

(a) When $2 \mid L$,

$$\Pi(\mathbb{D}_T) = (1 - \alpha) \left(2 - \frac{2}{\min\{L, n - L\}} \right).$$

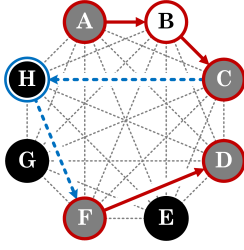


Figure 12: A path and its path trace for i.i.d. noise. Gray nodes are the endpoints of a revealed segment; white nodes are internal to a revealed segment; black nodes are not adjacent to any revealed edge.

(b) When $2 \nmid L$,

$$\Pi(\mathbb{D}_T) = (1 - \alpha) \left(2 - \frac{2}{L+1} - \frac{2}{n-L+1} \right).$$

The tradeoffs have been proved by the discussions above. \square

A.3 Proof of Theorem 4.6

Let $\lambda = L + 1$ denote the number of nodes in the path. Define $Q \triangleq \bigcup_{P \in \mathcal{P}} 2^P$, where 2^S denotes the class of subset of an arbitrary set S . Notice that the adversarial strategy \mathbb{A} has only one constraint – for every $Q \in \mathcal{Q}$, $\mathbb{A}[\cdot|Q]$ is a probability distribution over \mathcal{V} , while $\mathbb{A}[\cdot|Q_1]$ is independent with $\mathbb{A}[\cdot|Q_2]$ for $Q_1 \neq Q_2$. Hence, we can divide \mathbb{A} into many separate distributions with a small sample space \mathcal{V} .

Beginning with definition of privacy, we use a trick of comparing minimum and mean.

$$\begin{aligned} \Pi(\mathbb{D}_T) &= 1 - \sup_{\mathbb{A}} \min_{P \in \mathcal{P}} \sum_{Q \subseteq P} \mathbb{A}[\partial P|Q] \mathbb{D}_T[Q|P] \\ &\geq 1 - \sup_{\mathbb{A}} \frac{1}{|\mathcal{P}|} \sum_{P \in \mathcal{P}} \sum_{Q \subseteq P} \mathbb{A}[\partial P|Q] \mathbb{D}_T[Q|P] \end{aligned} \quad (\text{A.5})$$

$$\begin{aligned} &= 1 - \frac{1}{|\mathcal{P}|} \sup_{\mathbb{A}} \sum_{Q \in \mathcal{Q}} \alpha^{|Q|} (1 - \alpha)^{L-|Q|} \sum_{P \in \mathcal{P}, P \supset Q} \mathbb{A}[\partial P|Q] \\ &\triangleq 1 - \sum_{Q \in \mathcal{Q}} \frac{(n - \lambda)! \alpha^{|Q|} (1 - \alpha)^{L-|Q|}}{n!} \sup_{\mathbb{A}[\cdot|Q]} \sum_{v \in \mathcal{V}} \mathbb{A}[v|Q] Z(v, Q). \end{aligned} \quad (\text{A.6})$$

(A.6) ended with substitution $Z(v, Q) = |\{P \in \mathcal{P} | Q \subseteq P, v \in \partial P\}|$. Since Q is a path trace of P , it consists of several disconnected segments, where each segment consists of one or more edges connected end to end. Intuitively, a segment has two end nodes and zero or more intermediate nodes. The end nodes of segments are called **gray nodes**, and the intermediate nodes are called **white nodes**. The rest of the nodes in the network are called **black nodes**. Expressing these as sets, we let g_Q , w_Q and b_Q denote the sets of gray, white and black nodes given path trace Q . An example of segments and the aforementioned colors are shown in Figure 12.

The colors of nodes are decided by Q consisting of disconnected segments. Assume Q has $h_Q \geq 1$ segments. Furthermore, let k_Q denote the number of *internal* black nodes, i.e. the black nodes

on the original path. Relatively, *external* black nodes are the nodes out of the original path. Now the number of white nodes equals $\lambda - 2h_Q - k_Q$ and that of external black nodes equals $n - \lambda$. The value of $Z(v, Q)$ is discussed based on the color of v .

- (1) If v is a white node, it could never be an end node of a path, so $Z(v, Q) = 0$ for all $v \in w_Q$.
- (2) If v is a gray node, we first deal with the case that v is a source node of some segment σ_0 , where the other segments are denoted by σ_1 through σ_{h_Q-1} . Each original path with source node v has a permutation of the rest L nodes, which is uniquely mapped to a combination of the following options.
 - Order of segments on the path. There are $(h_Q - 1)!$ ways to permute q_1 through q_{n-1} .
 - Distribution of black nodes in the gaps between consecutive segments, or in the extension of the last segment. There are $\binom{h_Q + k_Q - 1}{k_Q}$ different ways to distribute the slots for black nodes.
 - Permutation of black nodes filling into the slots. Without regard of the position of the slots, there are $(n - \lambda + k_Q)! / (n - \lambda)!$ different permutations.

These options are independent of each other, so the multiplication rule applies. The analysis for v being a destination node of a segment is identical. It follows that for all $v \in g_Q$,

$$Z(v, Q) = \frac{(h_Q + k_Q - 1)!(n - \lambda + k_Q)!}{k_Q!(n - \lambda)!}. \quad (\text{A.7})$$

- (3) If v is a black node, we must assume $k_Q \geq 1$. We first deal with the case that v is a source node of the path. Similarly we discuss the following options.
 - Order of segments. There are $h_Q!$ different orders.
 - Distribution of the remaining $k_Q - 1$ slots for black nodes. There are $\binom{h_Q + k_Q - 1}{k_Q - 1}$ different distributions.
 - Permutation of black nodes filling into the slots. There are $(n - \lambda + k_Q - 1)! / (n - \lambda)!$ different permutations.
- The analysis for v being a destination node is identical. Considering v could be both source nodes and a destination nodes of different paths, for all $v \in b_Q$,

$$Z(v, Q) = \begin{cases} \frac{2(h_Q + k_Q - 1)!(n - \lambda + k_Q - 1)!}{(k_Q - 1)!(n - \lambda)!}, & k_Q \geq 1; \\ 0, & k_Q = 0. \end{cases} \quad (\text{A.8})$$

$Z(v, Q)$ depends only on the color of v , i.e. the set v belongs to. We may use $Z_g(Q)$ and $Z_b(Q)$ to denote $Z(v, Q)$ for an arbitrary $v \in g_Q$ and $v \in b_Q$, respectively. Starting with the LP in (A.6),

$$\begin{aligned} &\sup_{\mathbb{A}[\cdot|Q]} \sum_{v \in \mathcal{V}} \mathbb{A}[v|Q] Z(v, Q) \\ &= \sup_{\mathbb{A}[\cdot|Q]} \left[Z_g(Q) \sum_{u \in g_Q} \mathbb{A}[u|Q] + Z_b(Q) \sum_{v \in b_Q} \mathbb{A}[v|Q] \right] \\ &= \max \{ Z_g(Q), Z_b(Q) \} \\ &= \frac{(h_Q + k_Q - 1)!(n - \lambda + k_Q)!}{(n - \lambda)! k_Q!} \psi(k_Q), \end{aligned}$$

where

$$\psi(k_Q) = \begin{cases} 1, & k_Q \leq n - \lambda; \\ \frac{2k_Q}{n - \lambda + k_Q}, & \text{otherwise.} \end{cases}$$

One of the maximizers \mathbb{A}_I of the LP could be written as

$$\mathbb{A}_I[v|Q] = \begin{cases} \frac{\mathbb{I}[v \in g_Q]}{2h_Q}, & k_Q \leq n - \lambda; \\ \frac{\mathbb{I}[v \in b_Q]}{n - \lambda + k_Q}, & \text{otherwise.} \end{cases}$$

Explicitly, when the adversary sees balance updates on path trace Q , it picks a color from gray and black, and randomly chooses a node of that color. The choice of color depends on whether $k_Q \leq n - \lambda$. Recall that k_Q is the number of internal black nodes, and $n - \lambda$ is the number of external black nodes.

Let $f(\mathbb{A}, P) \triangleq \sum_{Q \subseteq P} \mathbb{A}[\partial P|Q] \mathbb{D}_I[Q|P]$. Based on the symmetry of \mathbb{A}_I , it's easy to confirm that when substituting the supremum over \mathbb{A} with \mathbb{A}_I in (A.5), it will make the inequality tight. Let \mathbb{U} denote the uniform distribution over \mathcal{P} . Now we obtain

$$\begin{aligned} \sup_{\mathbb{A}} \min_{P \in \mathcal{P}} f(\mathbb{A}, P) &\leq \sup_{\mathbb{A}} \mathbb{E}_{P \sim \mathbb{U}} f(\mathbb{A}, P) \\ &= \mathbb{E}_{P \sim \mathbb{U}} f(\mathbb{A}_I, P) = \min_{P \in \mathcal{P}} f(\mathbb{A}_I, P) \\ &\leq \sup_{\mathbb{A}} \min_{P \in \mathcal{P}} f(\mathbb{A}, P). \end{aligned}$$

Hence, (A.5) is actually an equality, and

$$\mathbb{A}_I \in \operatorname{argsup}_{\mathbb{A}} \min_{P \in \mathcal{P}} \sum_{Q \subseteq P} \mathbb{A}[\partial P|Q] \mathbb{D}_I[Q|P].$$

This means \mathbb{A}_I is an optimal adversarial strategy for i.i.d. noise \mathbb{D}_I and current routing scheme. The proof will be wrapped up with a final computation of $\Pi(\mathbb{D}_I)$ based on the optimal \mathbb{A}_I . Since $\min_{P \in \mathcal{P}} f(\mathbb{A}_I, P) = \mathbb{E}_{P \sim \mathbb{U}} f(\mathbb{A}_I, P)$, for an arbitrary $P' \in \mathcal{P}$,

$$\min_{P \in \mathcal{P}} f(\mathbb{A}_I, P) = f(\mathbb{A}_I, P').$$

Immediately,

$$\Pi(\mathbb{D}_I) = 1 - \sum_{Q \subseteq P'} \alpha^{|Q|} (1 - \alpha)^{L - |Q|} \mathbb{A}_I[\partial P'|Q]. \quad (\text{A.9})$$

Let v_s and v_d denote the source and destination of path P' , respectively. For a particular Q with $h \geq 1$ segments and k internal black nodes, we have $|Q| = \lambda - h - k$. Now we discuss the colors of v_s and v_d , depending on Q .

(1) If both are black, then

$$\mathbb{A}_I[v_s|Q] = \mathbb{A}_I[v_d|Q] = \frac{\mathbb{I}[k > n - \lambda]}{n - \lambda + k}.$$

Because the path is given, the number of path traces with both black ends equals the number of arrangements of slots for black nodes and white nodes. In this case, there are $h + 1$ gaps for $k - 2$ black nodes, and h gaps for $\lambda - 2h - k$ white nodes. Hence,

$$|\{Q \subseteq P | v_s, v_d \in b_Q\}| = \binom{h + k - 2}{k - 2} \binom{\lambda - h - k - 1}{h - 1}.$$

(2) If v_s is black and v_d is gray, then

$$\mathbb{A}_I[v_s|Q] = \frac{\mathbb{I}[k > n - \lambda]}{n - \lambda + k}, \quad \mathbb{A}_I[v_d|Q] = \frac{\mathbb{I}[k \leq n - \lambda]}{2h}.$$

Similarly, we find the number of path traces Q by finding the number of ways to put $k - 1$ slots of black nodes into h gaps, and $\lambda - 2h - k$ slots of white nodes into h gaps. Hence,

$$|\{Q \subseteq P | v_s \in b_Q, v_d \in g_Q\}| = \binom{h + k - 2}{k - 1} \binom{\lambda - h - k - 1}{h - 1}.$$

(3) If v_s is gray and v_d is black, by symmetry,

$$\mathbb{A}_I[v_s|Q] = \frac{\mathbb{I}[k \leq n - \lambda]}{2h}, \quad \mathbb{A}_I[v_d|Q] = \frac{\mathbb{I}[k > n - \lambda]}{n - \lambda + k},$$

$$|\{Q \subseteq P | v_s \in g_Q, v_d \in b_Q\}| = \binom{h + k - 2}{k - 1} \binom{\lambda - h - k - 1}{h - 1}.$$

(4) If both are gray, then

$$\mathbb{A}_I[v_s|Q] = \mathbb{A}_I[v_d|Q] = \frac{\mathbb{I}[k \leq n - \lambda]}{2h},$$

$$|\{Q \subseteq P | v_s \in g_Q, v_d \in b_Q\}| = \binom{h + k - 2}{k} \binom{\lambda - h - k - 1}{h - 1}.$$

The case $k < 2$ is not specified as $\binom{M}{N} = 0$ when $M < 0 \leq N$.

After the above discussion, we may conclude that for a particular Q , its term in the summation depends only on its h, k and the color of v_s and v_d . Therefore, the 2^λ terms in the original summation (A.9) is merged into $\text{Poly}(n)$ terms as below.

$$\begin{aligned} &1 - \Pi(\mathbb{D}_I) - \frac{2(1 - \alpha)^L}{n} \\ &= \sum_{h=1}^{\lfloor \lambda/2 \rfloor} \sum_{k=0}^{\lambda - 2h} \alpha^{\lambda - h - k} (1 - \alpha)^{h + k - 1} \cdot \binom{\lambda - h - k - 1}{h - 1} \cdot 2 \cdot \\ &\quad \left\{ \binom{h + k - 2}{k - 2} \frac{\mathbb{I}[k > n - \lambda]}{n - \lambda + k} \right. \\ &\quad \left. + \binom{h + k - 2}{k - 1} \left[\frac{\mathbb{I}[k > n - \lambda]}{n - \lambda + k} + \frac{\mathbb{I}[k \leq n - \lambda]}{2h} \right] \right. \\ &\quad \left. + \binom{h + k - 2}{k} \frac{\mathbb{I}[k \leq n - \lambda]}{2h} \right\} \\ &= \sum_{h=1}^{\lfloor \lambda/2 \rfloor} \sum_{k=0}^{\lambda - 2h} \alpha^{\lambda - h - k} (1 - \alpha)^{h + k - 1} \cdot \binom{\lambda - h - k - 1}{h - 1} \cdot 2 \cdot \\ &\quad \left\{ \binom{h + k - 1}{k - 1} \frac{\mathbb{I}[k > n - \lambda]}{n - \lambda + k} + \binom{h + k - 1}{k} \frac{\mathbb{I}[k \leq n - \lambda]}{2h} \right\} \\ &= \sum_{h=1}^{\lfloor \lambda/2 \rfloor} \sum_{k=0}^{\lambda - 2h} \alpha^{\lambda - h - k} (1 - \alpha)^{h + k - 1} \binom{\lambda - h - k - 1}{h - 1} \frac{\psi(k)}{h + k} \binom{h + k}{h} \\ &= \sum_{t=1}^{\lambda - 1} \frac{\alpha^{\lambda - t} (1 - \alpha)^{t - 1}}{t} \sum_{h=1}^{\min\{t, \lambda - t\}} \binom{t}{t - h} \binom{\lambda - t - 1}{h - 1} \psi(t - h). \end{aligned} \quad (\text{A.10})$$

(A.10) is the polynomial-time algorithm of computing $\Pi(\mathbb{D}_I)$. The tradeoff relationships of different settings of (n, λ) is shown in Figure 7. Because of $\psi(t - h)$, the summation above is difficult to simplify. Thus, we apply $\psi(t - h) \leq 2$ and provide a lower bound for privacy metric.

$$1 - \Pi(\mathbb{D}) - \frac{2(1 - \alpha)^L}{n}$$

$$\begin{aligned}
&\leq 2 \sum_{t=1}^{\lambda-1} \frac{\alpha^{\lambda-t}(1-\alpha)^{t-1}}{t} \sum_{h=1}^{\min\{t, \lambda-t\}} \binom{t}{t-h} \binom{\lambda-t-1}{h-1} \\
&= 2 \sum_{t=1}^{\lambda-1} \frac{\alpha^{\lambda-t}(1-\alpha)^{t-1}}{t} \binom{\lambda-1}{t-1} \\
&= \frac{2}{\lambda} \sum_{t=1}^{\lambda-1} \alpha^{\lambda-t}(1-\alpha)^{t-1} \binom{\lambda}{t} \\
&= \frac{2}{\lambda(1-\alpha)} \left[1 - \alpha^\lambda - (1-\alpha)^\lambda \right].
\end{aligned}$$

The lower bound in (4.6) is justified. \square

B SIMULATION RESULTS

To observe the effects of network size, the source and destination of each transaction are still drawn uniformly, and the values of transactions still follow Pareto distribution $\Psi(1.16, 1000)$. To generate smaller versions of the Lightning network, we snowball sample the full-sized graph until reaching the desired size. For each network size, we sample 100 networks, and the average density of both Erdős-Rényi and LND networks are matched.

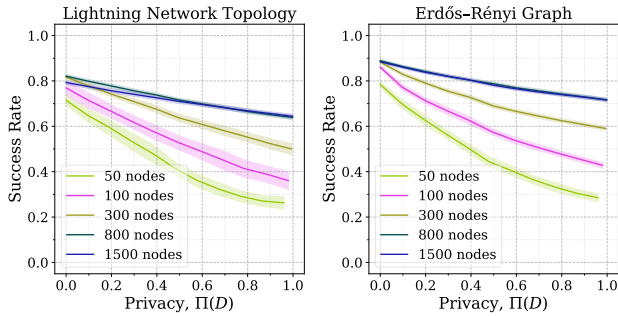


Figure 13: Privacy-Success rate tradeoff curves for different graph sizes.

The tradeoff curves are shown in Figure 13. When the size is small, there is high variance in network topology of LND, which leads to high variance in success rates. As the network size increases, the privacy-success rate tradeoff becomes insensitive to these variations. Moreover, we observe that success rate increases. This may be because as more nodes are added, there are more paths for transactions to traverse, which gives additional robustness to link imbalance.

B.1 Data distributions and workloads

Figure 14 illustrates the pdfs of the Pareto distributions used in our experiments. Notice that Pareto distributions have a minimum transaction value, and are also heavy-tailed.

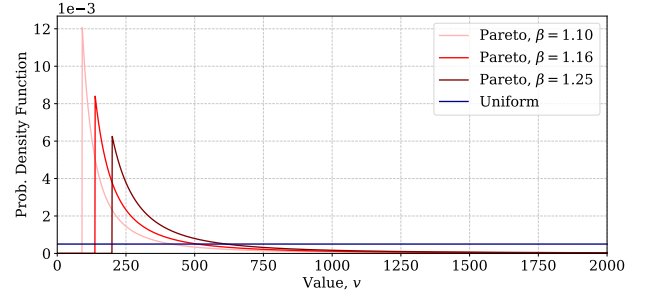


Figure 14: Pareto distribution pdfs for different parameter settings.

Our experiments use a snapshot of the real Lightning network topology, illustrated in Figure 15. The graph has many nodes of degree 1 or 2, with several large hubs that are well-connected. This is qualitatively different from the synthetic ER graphs we also used in experiments.

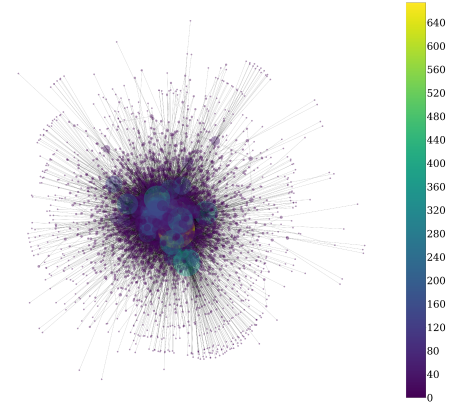


Figure 15: Snapshot of the Lightning network topology from December 28, 2018. Node sizes are scaled proportionally to their degree in the graph.